

Research Article

Comparison of Tidalites in Siliciclastic, Carbonate, and Mixed Siliciclastic-Carbonate Systems: Examples from Cambrian and Devonian Deposits of East-Central Iran

Hamed Zand-Moghadam, Reza Moussavi-Harami, Asadollah Mahboubi, and Hoda Bavi

Department of Geology, Faculty of Science, Ferdowsi University of Mashhad, Azadi Square, University Campus, P.O. Box 917751436, Mashhad 91779 48953, Iran

Correspondence should be addressed to Hamed Zand-Moghadam; zand1883@yahoo.com

Received 10 April 2013; Accepted 20 May 2013

Academic Editors: M. Ginter, J. Golonka, M. C. Melinte-Dobrinescu, and J. P. Suc

Copyright © 2013 Hamed Zand-Moghadam et al. This is an open access article distributed under the Creative Commons Attribution License, which permits unrestricted use, distribution, and reproduction in any medium, provided the original work is properly cited.

For the comparison of lithofacies in siliciclastic, carbonate, and mixed siliciclastic-carbonate tidal systems, three successions including Top Quartzite (Lower-Middle Cambrian), Deranj Formation (Upper Cambrian), and Padeha Formation (Lower-Middle Devonian) in the north of Kerman and Tabas regions (SE and E central Iran) were selected and described, respectively. Lithofacies analysis led to identification of 14 lithofacies (Gcm, Gms, Gt, Sp, St, Sh, Sl, Sr, Sm, Se, Sr(Fl), Sr/Fl, Fl(Sr), and Fl) and 4 architectural elements (CH, LA, SB, and FF) in the Top Quartzite, 7 lithofacies (Dim, Dp, Dr, Ds, Dl, Dr/Dl, and Fcl) and 2 architectural elements (CH, CB) in the Deranj Formation, and 17 lithofacies (Sp, St, Sh, Sl, Sr, Se, Sr(Fl), Sr/Fl, Fl(Sr), Fl, Dr, Ds, Sr/Dl, El, Efm, Efl, and Edl) and 5 architectural elements (CH, LA, SB, FE, and EF) in the Padeha Formation that have been deposited under the influence of tides. The most diagnostic features for comparison of the three tidalite systems are sedimentary structures, textures, and fabrics as well as architectural elements (lithofacies association). The CH element in siliciclastics has the highest vertical thickness and the least lateral extension, while in the carbonate tidalites, it has the least vertical thickness and the most lateral extension compared to in other systems.

1. Introduction

The term *Tidalites* was introduced by Klein [2, 3] to designate a new process for sedimentary facies, deposited by tidal currents [4]. It is now applied to all sediments and sedimentary structures that have accumulated under the influence of tides [5]. Three subenvironments, including subtidal, intertidal, and supratidal, can be distinguished on the basis of sedimentary structures, textures, lithologies, and vertical successions of such facies. Tidalites are somewhat synonymous with peritidal sediments, formed near the tidal zone [6–8]. Although tidalites are common in passive margins, they also occur in failed rifts, intracratonic, foreland, back-arc/fore-arc, and pull-apart basins (e.g., [9–11]). Sedimentary structures are the most diagnostic features used in analyzing and describing tidal flat deposits. These sedimentary lines of evidence reflect different types of physical, chemical, and

biochemical conditions in tidal facies. In another word, each different sedimentary structure is representative of one particular subenvironment within the tidal zone [5, 11]. Although sedimentary structures in both siliciclastic and carbonate tidal zones are similar, they differ in their abundance. The mixed siliciclastic-carbonate deposits in the ancient shallow and coastal marine environments contain the most sedimentary structures. The aim of this paper is to discuss and compare the petrography and lithofacies characteristics of tidalites in three siliciclastic, carbonate, and mixed siliciclastic-carbonate depositional systems in order to have a better understanding of tidal facies in such sedimentary systems. In this research, in central Iran, the Lower-Middle Cambrian (Top Quartzite) sediments east of Zarand in Kerman area were analyzed to study tidalite from a siliciclastic depositional system (Figures 1 and 2). The Upper Cambrian deposits (equivalent of the Deranj

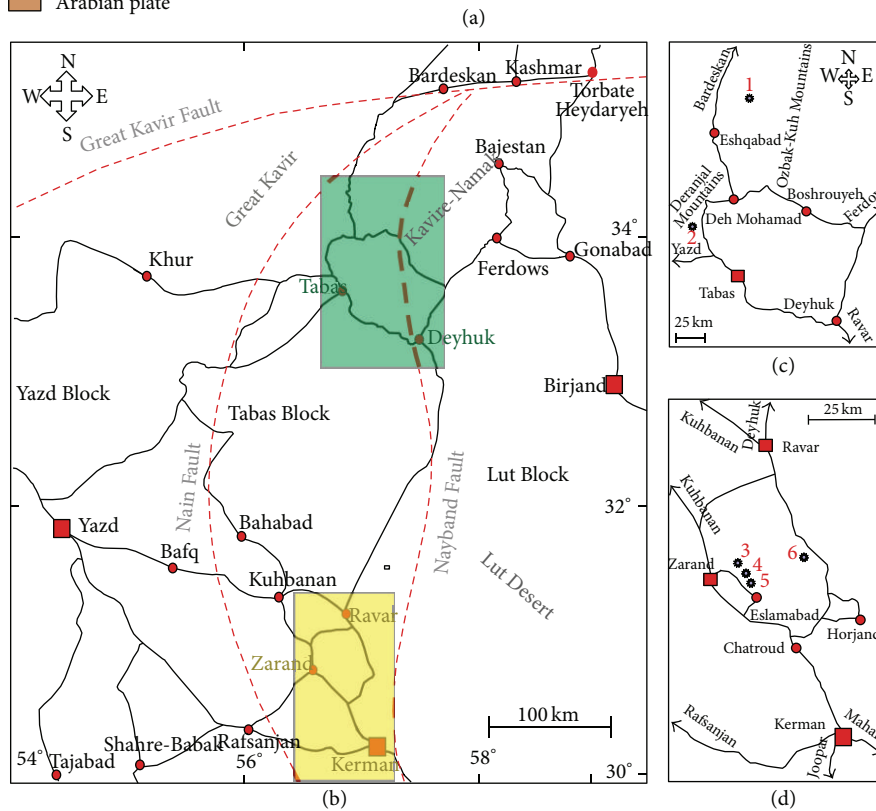
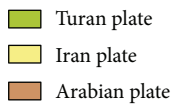


FIGURE 1: Locality map of the study area and measured stratigraphic sections in east-central Iran. (a) Structural units of Iran (modified from Alavi [16]). (b) Close-up view of white square, east-central Iran (modified from Wilmsen et al. [17]). (c) The study area shaded in green on (b) shows the locations of measured sections in north of Tabas ((1) Ozbak-Kuh, (2) Dahane-Kalot). (d) The study area shaded in yellow on (b) shows the locations of measured sections in NW Kerman ((3) Gazuieh, (4) Gatkuieh, (5) Dahuieh, (6) Sarashk).

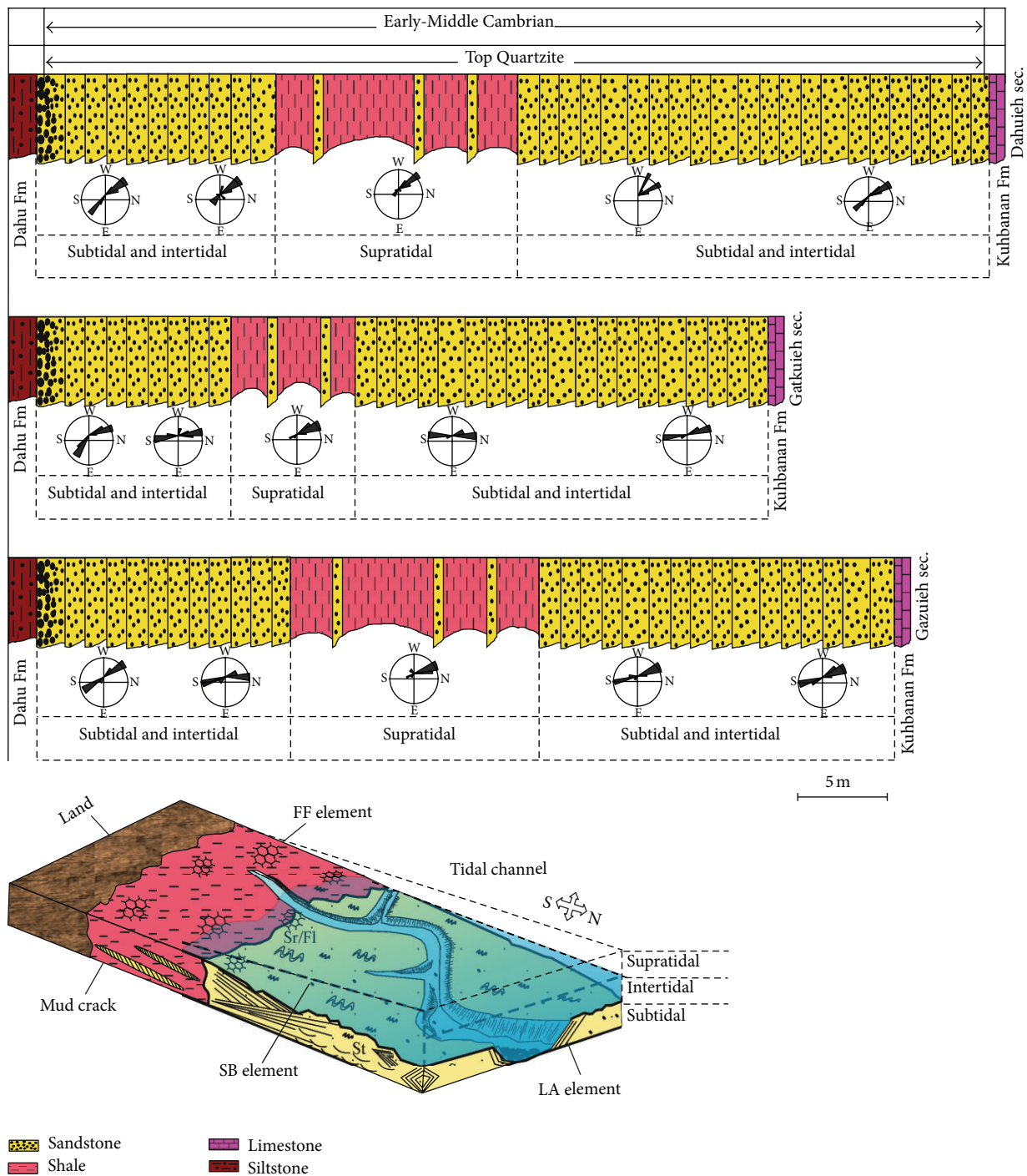


FIGURE 2: Lithostratigraphic columns and 3D depositional model of the siliciclastic tidalites (Top Quartzite) in the East Zarand, NW Kerman. Datum line is base of the Top Quartzite.

Formation) in the same area were also studied for facies interpretations of tidalites in carbonate systems (Figures 1 and 3). In northern Tabas and northwestern Kerman, three stratigraphy sections of the Padeha Formation were selected and described for analyzing facies characteristics of tidalites in a mixed siliciclastic-carbonate depositional system (Figures 1 and 4). Evaporates are also present in these systems.

2. Geological Setting

The study area is located in the central part of the Central-East Iranian Microcontinent (CEIM; [12]). The CEIM, together with central Iran and the Alborz Mountains, forms the Iran Plate, which occupies a structural key position in the Middle-Eastern Tethysides [13]. The CEIM consists of three north-south-oriented structural units, called the Lut, Tabas, and

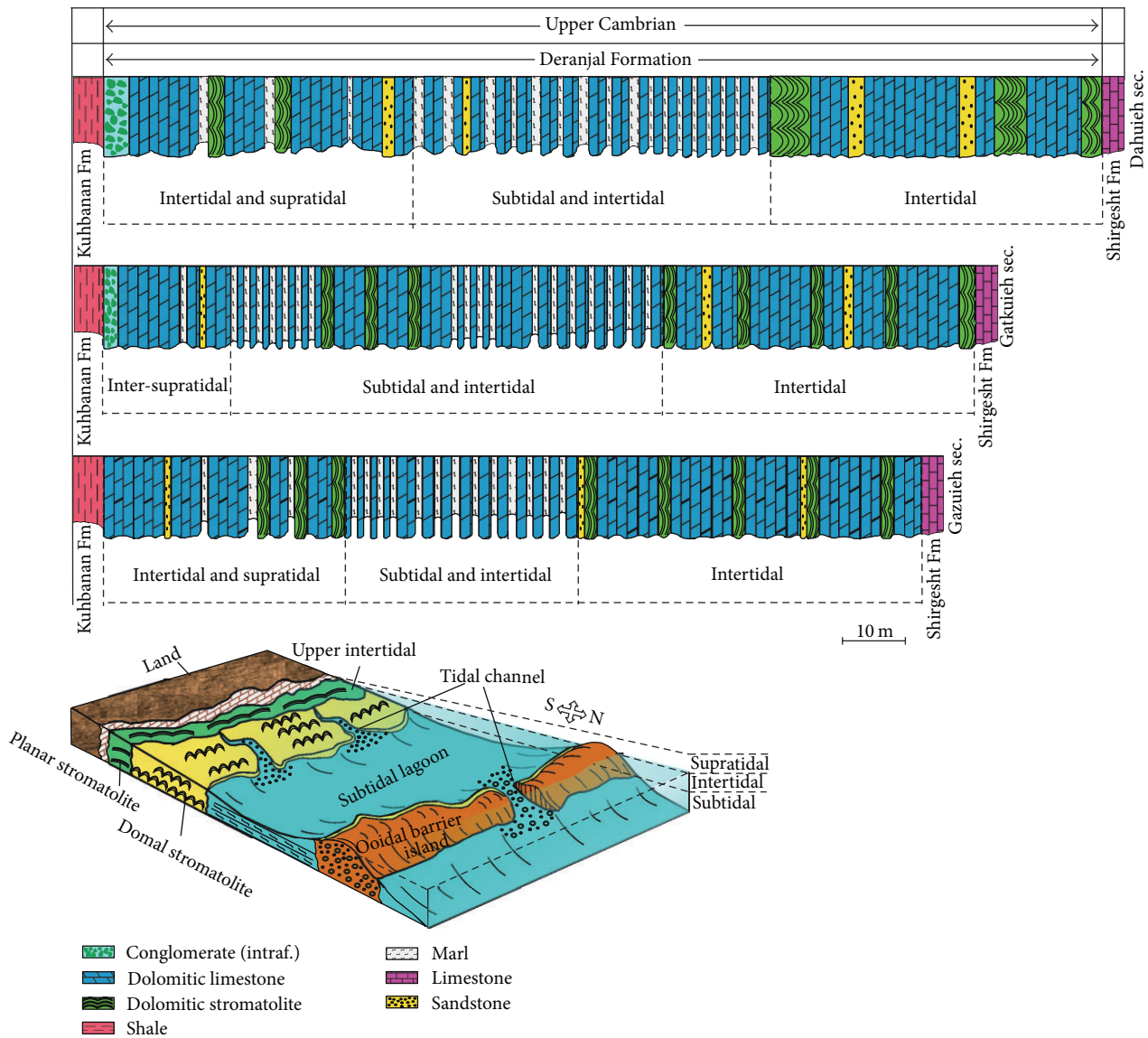


FIGURE 3: Lithostratigraphic columns and 3D depositional model of the carbonate tidalites (Deranj Formation) in the East Zarand, NW Kerman. Datum line is base of the Deranj Formation.

Yazd Blocks (Figure 1), which are now aligned from east to west, respectively [14]. The study area is located in the north and south parts of Tabas Block. The rock succession exposed in this area includes all systems from the Pre-Cambrian up to recent. This Block is bounded by the Great Kavir Fault in the north, the Naini Fault (Nain-Baft Fault) in the west and southwest, and the Nayband Fault in the east (Figure 1). An important characteristic of the Tabas Block is that it bears a complete succession of Paleozoic rocks that is incomplete in other parts of Iran [14, 15].

This study focuses on the Cambrian and Early-Middle Devonian rocks in the south and north of Tabas Block (Figure 1(c)). The basement of the Tabas Block consists of metamorphic complexes which contain volcanic, volcanoclastic, and pyroclastic rocks with marbles. This basement is

similar to the Arabian Proterozoic basement (Pan-African basement) [18, 19]. The Late Precambrian-Lower Cambrian successions of this block include successions of basic lavas, sandstone, and evaporite-dolomite (Rizu and Dezu series) which is attributed to a rifting system by Aghanabati [19].

From a regional point of view, Paleozoic deposits are widespread throughout the Arabian and Iranian terrains. Facies analysis for Cambrian to Devonian rocks in the Tabas Block indicates that they were mostly deposited in shallow marine environments (e.g., [18, 20]). The paleogeographic map of the Cambrian to Devonian of Arabia and Iran shows that its adjoining plates formed a broad continental shelf on the northern margin of the Gondwana supercontinent, which bordered on the Paleo-Tethys Ocean (e.g., [19–23]). It should be noted, however, that Lasemi [24] argues that

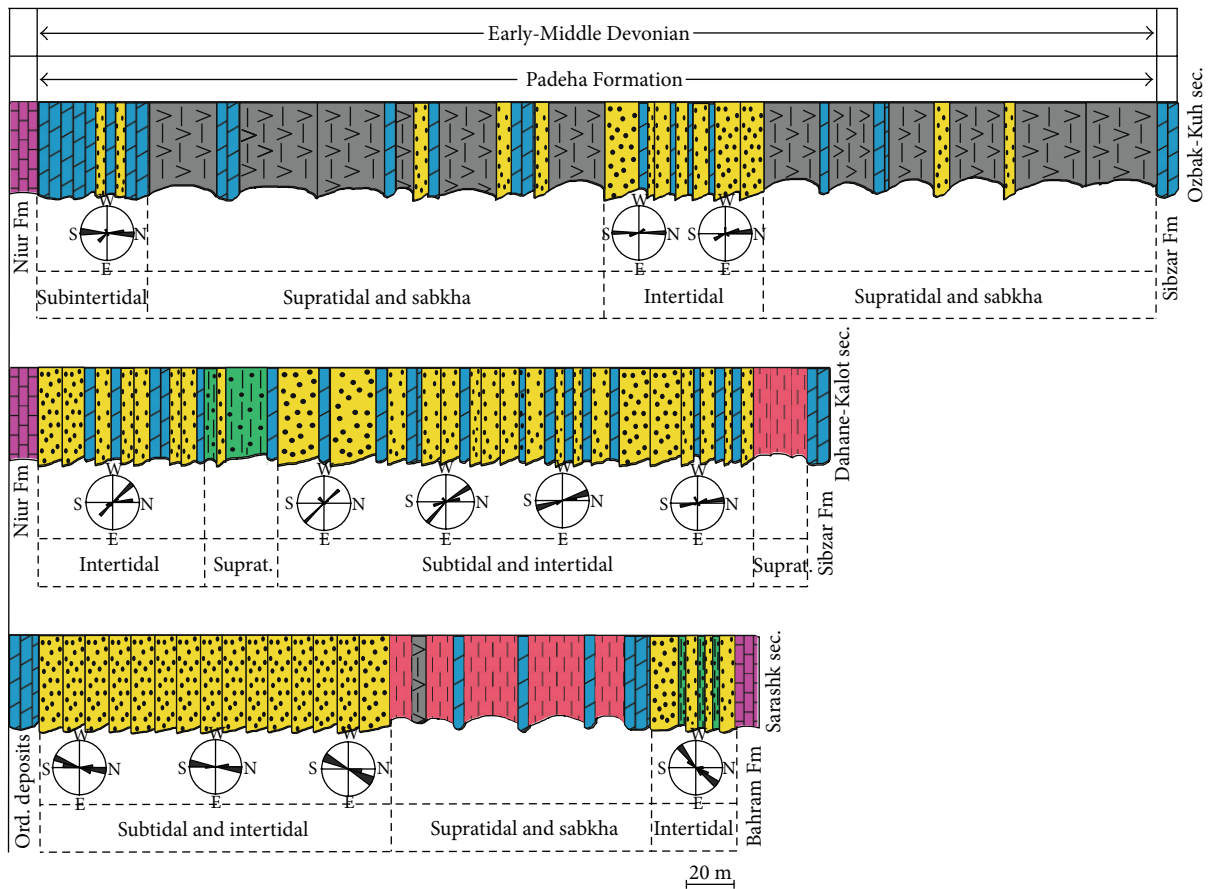


FIGURE 4: Lithostratigraphic columns and 3D depositional model of the mixed tidalites (Padeha Formation) in central Iran. Datum line is base of the Padeha Formation.

the Precambrian-Cambrian sedimentary facies indicate the existence of an ocean older than the Paleo-Tethys in Iran, which is named the Proto Paleo-Tethys.

Several formations were introduced from the Cambrian succession in central Iran. The Dahu Formation (Lower Cambrian), Top Quartzite Unit (Lower-Middle Cambrian), Kuhbanan Formation (Middle Cambrian), and Deranj Formation (Upper Cambrian) are the most widespread in Iran, especially at northern Kerman. Cambrian sedimentary rocks are exposed in most parts of Iran except in

the north-east (Kopeh-Dagh region). The Padeha Formation (Lower-Middle Devonian) is part of Devonian succession that has an extensive lateral expansion in Iran. Wendt et al. [25] believed that the Padeha Formation is mainly deposited in a siliciclastic shelf, especially shallow marine environment.

3. Materials and Methods

This study is based on petrography and facies descriptions from nine stratigraphic sections selected from the Cambrian

and Devonian deposits in eastern and southeastern parts of central Iran. A total number of 780 thin sections were prepared from approximately 980 rock samples for the lab analysis. For carbonates, thin sections were stained with red alizarin solution in order to differentiate calcite and dolomite minerals [26]. The identified facies were classified into siliciclastic and carbonate lithofacies on the basis of field observations, microscopic, and lab analysis. The description of the facies is based on facies codes presented by Miall [1]. New facies codes are also determined and added. The siliciclastic petrofacies and carbonate microfacies are classified and described on the basis of Folk's [27] and Dunham's [28] classifications, respectively. The petrography features and the mineralogical composition of microstructures were analyzed using SEM-EDX in the central laboratory of Ferdowsi University of Mashhad. 180 oriented sedimentary structures were measured from the siliciclastic sediments for paleocurrents analysis.

4. Results

4.1. Siliciclastic Tidalites. These types of tidalites are identified in the Lower-Middle Cambrian siliciclasts of the Top Quartzite sediments that overlie the fluvial deposits of the Dahu Formation [29] during a falling of relative sea level change. Huckriede et al. [15] described the Top Quartzite and the red sediments of the Dahu Formation as the Dahu series. The lithofacies and the depositional model of the Top Quartzite succession were studied by Zand-Moghadam et al. [30] in three stratigraphic sections measured in Gazuieh (with 47 m thickness located at 5 km east of Zarand), Gatkuieh (with 43 m thickness located at 15 km southeast of Zarand), and Dahuieh (with 53 m thickness located at 20 km southeast of Zarand) in the southeast of central Iran. These sediments are considered as tidalites formed in a siliciclastic system (Figure 2).

The field studies revealed that the Top Quartzite siliciclastic succession can be divided into three lithostratigraphic units. The lower part consists of conglomerate and sandstone. Mudstone and sandstone comprise the middle part of the succession, while the upper part consists mainly of sandstone. The lower and upper parts of the Top Quartzite succession are composed of conglomerate (Gcm, Gms, Gt), sandstone (Sp, St, Sh, Sl, Sr, Sm, Se), and interbedded sandstone-mudstone (Sr(Fl), Sr/Fl) lithofacies (Table 1). The most diagnostic sedimentary structures in these lithofacies include wave, current, and interference ripples (Table 2; Figures 5(a) and 5(b)), planar and trough cross-beds, herringbone cross-beds with bimodal pattern of paleocurrent (Figure 6(a)), reactivation surfaces, flaser and wavy bedding (Figure 7(c)), polygonal mud cracks, and some trace fossils (dominated by *Cruziana*).

On the basis of the identified lithofacies, three CH, LA, and SB elements, representative of tidal channel deposits and sand body macroforms, were recognized (Table 3, Figures 10 and 11). These elements were deposited in subtidal and intertidal subenvironments. The dominant petrofacies are mature-super-mature quartzarenite and chertarenite. Also, textural inversion was identified in some of the lithofacies.

The middle parts of the Top Quartzite succession are composed of red-colored mudstones with dominant Fl lithofacies and other supratidal lithofacies such as sandstone (Sp, Sr, Sh, and Se) and interbedded sandstone-mudstone (Sr/Fl, Fl(Sr)) lithofacies. Most of the sedimentary structures in these lithofacies are polygonal mud cracks (Figures 8(a)–8(c)), raindrop imprints, wavy and lenticular beds, interference ripples, and planar cross-beds. The presence of such sedimentary structures resulted in identification of FF elements in this part. Siltstone and claystone are the dominant petrofacies of the supratidal lithofacies.

4.2. Carbonate Tidalites. The carbonate tidalites are described from the Upper Cambrian carbonate deposits in northwestern Kerman. These carbonate deposits comprise the upper lithostratigraphic unit of the Kuhbanan Formation and can be equivalent to the Deranjel Formation in Tabas area or correlated with the units 2 and 3 of the Mila Formation in the Alborz Mountains [31]. Therefore, based on the stratigraphic position, the Upper Cambrian carbonate deposits in northwestern Kerman can be assigned to the Deranjel Formation. The facies analysis and environmental interpretations of the carbonate deposits are focused on three measured stratigraphic sections in Gazuieh, Gatkuieh, and Dahuieh in the east and southeast of Zarand (Figures 1 and 3). The studied sections are 130 m, 140 m, and 160 m thick, respectively. Despite the wide dolomitization within the carbonate facies, the facies are easily describable and recognizable due to the well preservation of their original textures.

The field studies resulted in identification of dominant carbonate lithofacies such as Ds, Dl, Dr, and Dp. The Dl lithofacies completely consists of primary dolomites (Table 1). These lithofacies are intercalated with fine-grained marls (Flc lithofacies). Based on diverse morphologies of stromatolites within the Ds lithofacies, dome-shaped (Dsd) and planar stromatolites (Dsp) were recognized (Figures 9(a)–9(g)). Also, in the Dahuieh section, a coarse-grained (pebble-sized carbonate intraclasts) lithofacies (Dim) was identified. The poorly sorted and angular carbonate clasts are cemented with sparite and minor micrite. The most diagnostic sedimentary structures in carbonate tidalites are dominated by wavy and climbing ripples (Figures 5(d)–5(e)), planar, herringbone, and ripple cross-lamination (Figures 6(b)–6(d)), hummocky cross-beds, V-shaped mud cracks (Figure 8(d)), and diverse stromatolitic structures (Figures 9(a)–9(g)).

The microscopic analysis led to recognition of several carbonate microfacies such as dolomudstone, sandy dolomudstone, dolomitic lime mudstone, dolomitic stromatolitic boundstone, dolomitic peloidal packstone, and dolomitic intraclast-ooidal grainstone. Sparse sandstone (Sp, Sr, and Sh) lithofacies with low lateral distribution were also intercalated with the carbonate facies. The quartzarenite is the only siliciclastic petrofacies observed in the sandstone lithofacies.

The lithofacies analysis reflects the dominant role of tidal currents in deposition of the studied facies. Under this sedimentary condition, the dolomudstone, sandy dolomudstone (consisting of Dl lithofacies), and the boundstone

TABLE 1: Summary of characteristics of lithofacies (lithofacies codes modified after Miall [1]).

| Lithofacies | Code | Description | Petrography | Interpretation | Occurrence |
|----------------------------------------|--------|---------------------------------------------------------------------------------------------------|--------------------------------------|--------------------------------------------------------------------------------------------------------------------------------------------|-----------------------------------|
| Conglomerate | | | | | |
| Clast-supported | Gcm | Massive; granule- to pebble-sized clasts; oligomictic (chert) | Orthoconglomerate | Bedload transport lag deposits in tidal channels | Top Quartzite |
| Matrix-supported | Gms | Massive or crudely bedded; granule- to pebble-sized; oligomictic (chert) | Paraconglomerate | Bedload transport lag deposits in tidal channels | Top Quartzite |
| Trough cross-bedded | Gt | Granule- to pebble-sized; clasts bed thickness generally 1 to 2 m. | Paraconglomerate | Bedload transport tidal channel deposits | Top Quartzite |
| Sandstone | | | | | |
| Trough cross-bedded | St | Medium sand solitary or grouped; set thickness generally 2–30 cm | Quartzarenite, sometimes litharenite | 3D dunes and interference ripples movement; tidal channels | Top Quartzite Padeha and Deranjai |
| Planar cross-bedded | Sp | Coarse-fine sand; solitary or grouped; set thickness generally 5–50 cm; herringbone cross-bedding | Quartzarenite, sometimes litharenite | Transverse and linguoid bedforms (ripple or 2D dunes); grouped tabular sets with bipolar-bimodal paleocurrents representing tidal channels | Top Quartzite Padeha Fm |
| Horizontally bedded or laminated | Sh | Fine sand; set thickness generally 5–100 cm; sometimes with trace fossils | Quartzarenite | Planar bed lower and upper flow in tidal flat | Top Quartzite Padeha and Deranjai |
| Low-angle (<10) cross-bedded | Sl | Medium to fine sand; small wedge-shaped sets | Quartzarenite | Oscillation of wave swash and backwash in intertidal | Top Quartzite Padeha Fm |
| Rippled | Sr | Medium to fine sand wave and interference ripples set thickness generally 2–80 cm | Quartzarenite, sometimes litharenite | Deposition from traction current ripples with low indices (5–7) related to wave-induced currents in tidal flat | Top Quartzite Padeha and Deranjai |
| Massive | Sm | Medium sand and massive to crudely bedded | Quartzarenite | Gravity and turbulence currents | Top Quartzite |
| Scour pits | Se | Coarse-fine sand; base of Sp and Sh lithofacies; set thickness 1–10 cm | Muddy pebble quartzarenite | Scour fills in base of tidal channels | Top Quartzite Padeha Fm |
| Interbedded sandstones-mudstone | | | | | |
| Flaser bedded | Sr(Fl) | Lenticular mud interbeds sand | Quartzarenite-siltstone | Alternating strong and weak flows in intertidal | Top Quartzite Padeha Fm |
| Wavy bedded | Sr/Fl | Rippled sand interbeds mud | Quartzarenite-siltstone | Alternating strong and weak flows in upper intertidal | Top Quartzite Padeha Fm |
| Lenticular bedded | Fl(Sr) | Rippled sand lenses in mud | Quartzarenite-siltstone | Alternating strong and weak flows in upper intertidal-supratidal | Top Quartzite Padeha Fm |
| Mudstone | | | | | |
| Laminated or rippled | Fl | Often silt size 1-2 cm layers; sometimes with ripple and mud cracks | Siltstone; claystone | Deposition from traction current in upper intertidal and supratidal | Top Quartzite Padeha Fm |
| Laminated marl | Flc | Silt and clay size with carbonates planar laminate and cross-laminated | Silty lime mudstone | Low-energy environments (subtidal lagoon) | Deranjai Fm |
| Carbonate | | | | | |
| Massive | Dim | Carbonate intraclasts; pebble-sized; intraformational | Dolomitic intraclastic grainstone | Debris flow and turbulence currents in tidal channels | Deranjai Fm |

TABLE 1: Continued.

| Lithofacies | Code | Description | Petrography | Interpretation | Occurrence |
|-------------------------------------|-------|----------------------------------------------------------------------|----------------------------------------|---------------------------------------------------------------------|--------------------------|
| Planar cross-bedded | Dp | Sand-sized grains; herringbone cross-bedding | Dolomitic ooid grainstone to packstone | Tidal channel deposits in intertidal and subtidal | Deranjel Fm |
| Rippled | Dr | Wavy and climbing ripples; set thickness 0.1–0.8 m | Dolomitic ooid grainstone to packstone | Tidal channel deposits in intertidal and subtidal | Deranjel Fm |
| Laminated | Dl | Set thickness 0.1–2 m; sometimes with sand and mud | Dolomudstone; sandy dolomudstone | Deposited in tidal setting (often upper intertidal to supratidal) | Deranjel Fm Padeha Fm |
| Stromatolitic | Ds | Set thickness 0.5–3 m; sometimes with sand lenses | Dolomitic boundstone; dolomudstone | Deposited in tidal setting (often intertidal) | Deranjel Fm Padeha Fm |
| Flaser-wavy bedded | Dr/Dl | Lenticular calcilutite interbeds calcarenite; flaser and wavy bedded | Dolomitic grainstone; dolomudstone | Alternating strong and weak flows in intertidal setting | Deranjel Fm |
| Interbedded sandstones-dolomudstone | | | | | |
| Flaser-wavy bedded | Sr/Dl | Rippled sand interbeds laminated dolomudstone | Quartzarenite-dolomudstone | Alternating strong and weak flows in upper intertidal to supratidal | Padeha Fm |
| Evaporate | | | | | |
| Laminated | El | Set thickness 0.2–1.5 m; enterolithic folding | Gypsum, sometimes anhydrite | Subaerial precipitation in sabkha or supratidal | Padeha Fm |
| Laminated or rippled | Efl | Evaporate interbeds mud; sometimes mud crocks, salt casts | Gysiferous mudstone | Subaerial-subaqueous precipitation in sabkha or supratidal | Padeha Fm |
| Massive | Efm | Evaporate patch in mud sometimes mud; cracks and rain spots | Gypsum-siltstone | Subaerial-subaqueous precipitation in sabkha or supratidal | Padeha Fm |
| Laminated and rippled | Edl | Evaporate interbeds dolomite | Gypsum-dolomudstone | Subaerial-subaqueous precipitation in sabkha or supratidal | Padeha Fm |

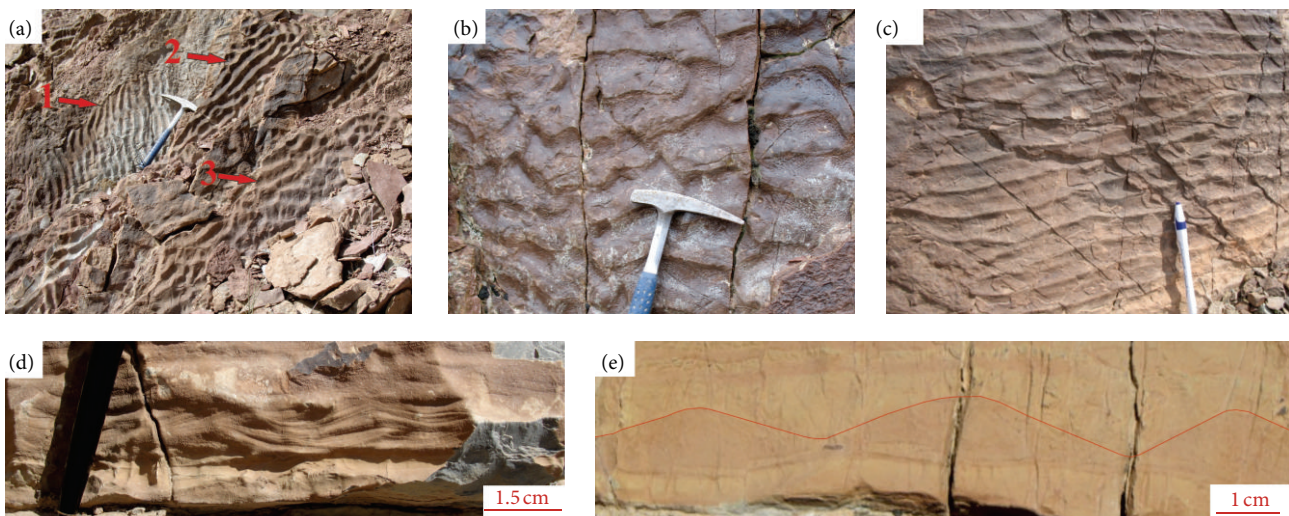


FIGURE 5: Comparison of ripple marks in Sr lithofacies. (a) Three types of ripples in the sandstones of Top Quartzite. (1) Double crest wavy ripples. (2) Wavy and current ripples. (3) Interference ripples. (b) Catenary crest of current ripples in the Top Quartzite sandstones. (c) Sinuous-straight crest of wavy ripples in sandstone of Padeha Formation. (d) and (e) Climbing and wavy ripples in the carbonate tidalites of Deranjel Formation.

TABLE 2: Comparison of sedimentary structures in the siliciclastic, carbonate, and mixed siliciclastic-carbonate tidalites. For more details see text.

| Sedimentary structures and fabrics | Siliciclastic tidalites (Top Quartzite Unit) | Mixed tidalites (Padeha Formation) | Carbonate tidalites (Deranjel Formation) | Petrofacies | Microfacies |
|------------------------------------|----------------------------------------------|------------------------------------|------------------------------------------|---------------|--------------|
| Normal graded bedding | ✓✓✓ | ✓✓✓ | ✓✓ | Qtz and Lit | Grst |
| Intraformational clasts | ✗ | ✓ | ✓✓✓ | Qtz | Intra Grst |
| Scour pits | ✓✓ | ✓ | ✓ | Qtz and Lit | Grst |
| Wavy ripples | ✓✓✓ | ✓✓✓ | ✓✓ | Qtz and Lit | Grst-Pkst |
| Current ripples | ✓✓ | ✗ | ✓ | Qtz and Lit | Wkst and Dol |
| Interference ripples | ✓✓✓ | ✓ | ✗ | Qtz and Lit | ✗ |
| Climbing ripples | ✗ | ✗ | ✓✓ | ✗ | Grst-Wkst |
| Trough cross-beds | ✓✓ | ✓ | ✓ | Qtz and Lit | Grst |
| Planar cross-beds | ✓✓✓ | ✓✓✓ | ✓ | Qtz and Lit | Grst-Pkst |
| Herringbone cross-beds | ✓✓✓ | ✓✓ | ✓ | Qtz | Grst-Pkst |
| Hummocky cross-beds | ✗ | ✓ | ✗ | Qtz | ✗ |
| Reactivation surfaces | ✓✓✓ | ✓✓✓ | ✓ | Qtz and Lit | Grst |
| Flaser bedding | ✓✓✓ | ✓✓✓ | ✓✓✓ | Qtz and Stst | Grst-Pkst |
| Wavy bedding | ✓✓✓ | ✓✓✓ | ✓✓ | Qtz and Stst | Grst-Wkst |
| Lenticular bedding | ✓✓✓ | ✓✓✓ | ✓ | Stst and Qtz | Dol |
| Polygonal mudcracks | ✓✓✓ | ✓✓ | ✗ | Stst and Clst | ✗ |
| V-shaped mudcracks | ✓✓✓ | ✓✓✓ | ✓ | Stst and Clst | Dol |
| Syneresis cracks | ✗ | ✓ | ✗ | Stst | ✗ |
| Raindrop imprints | ✓ | ✓ | ✗ | Stst and Clst | ✗ |
| Salt casts | ✗ | ✓✓ | ✗ | ✗ | Dol |
| Pseudomorph calcite | ✗ | ✓ | ✓ | ✗ | Dol |
| Entrolithic folding | ✗ | ✓ | ✗ | ✗ | Gyp and Any |
| Stromatolite structures | ✗ | ✓✓ | ✓✓✓ | ✗ | Dol and Bdst |
| Tepee structures | ✗ | ✓✓ | ✓ | ✗ | Dol |
| Fenestral fabric | ✗ | ✓ | ✓ | ✗ | Dol |
| Tracks and trails | ✓✓ | ✓✓ | ✓✓ | Qtz and Stst | Grst-Wkst |

Absent (✗) → Very common (✓✓✓), Lit: litharenite, Grst: grainstone, Dol: dolomudstone, Intra Grst: Intraclastic grainstone (pebble size), Stst: siltstone, Pkst: packstone, Gyp: gypsum, Bdst: Boundstone, Qtz: quartzarenite, Clst: claystone, Wkst: wackstone, Any: anhydrite.

(Dsp lithofacies) were deposited in the upper intertidal and supratidal subenvironment. The carbonate lithofacies (Dsd, Dr, and Dp) as well as sparse sandstone lithofacies (Sh, Sr, and Sp) were deposited in the intertidal zone and tidal channels reflecting CH and CB elements (Table 3). The fine-grained marl lithofacies (Flc) indicated that deposition may have taken place in subtidal lagoon [31].

4.3. Mixed Siliciclastic-Carbonate Tidalites. Based on the lithological diversity and the presence of different flow regimes in this depositional system, the mixed siliciclastic-carbonate tidalites contain the most diagnostic sedimentary signature. In the siliciclastic-carbonate systems, in addition to tidal influences, environments such as fluvial, estuaries, deltas, and wave current are effective in the type of sediments (e.g., [32]). However, the intensity of the tidal currents is the main factor in controlling the deposition of tidalites. In some of the studied sections, the sediments of the Padeha

Formation were deposited by tidal currents [33]. For example, in the type section (the Ozbak-Kuh section), the Dahane-Kalot in north of Tabas, and the Sarashk sections in northeast Kerman (Figure 1), the sediments of this formation consist of tidalites, reflecting tidal subenvironments and conditions.

The Padeha Formation was first measured and introduced by Ruttner et al. [34] in Ozbak-Kuh Mountain, north of Tabas, and was described as the second formation within the Goshkamar Group (Niur and Padeha Formation). The sedimentary succession of the Padeha Formation comprises siliciclasts, dolomites, and evaporites. The formation overlies the carbonate settings of the Niur Formation and is overlain by the carbonate deposits of the Sibzar and Bahram Formations. The Padeha Formation has been assigned to Lower-Middle Devonian based on its stratigraphic position [25, 35, 36] and can be considered as an equivalent of the Lower Devonian red siliciclastic sediments that are extended widely in other regions in the world. Due to different deposition conditions and the distances between the studied sections

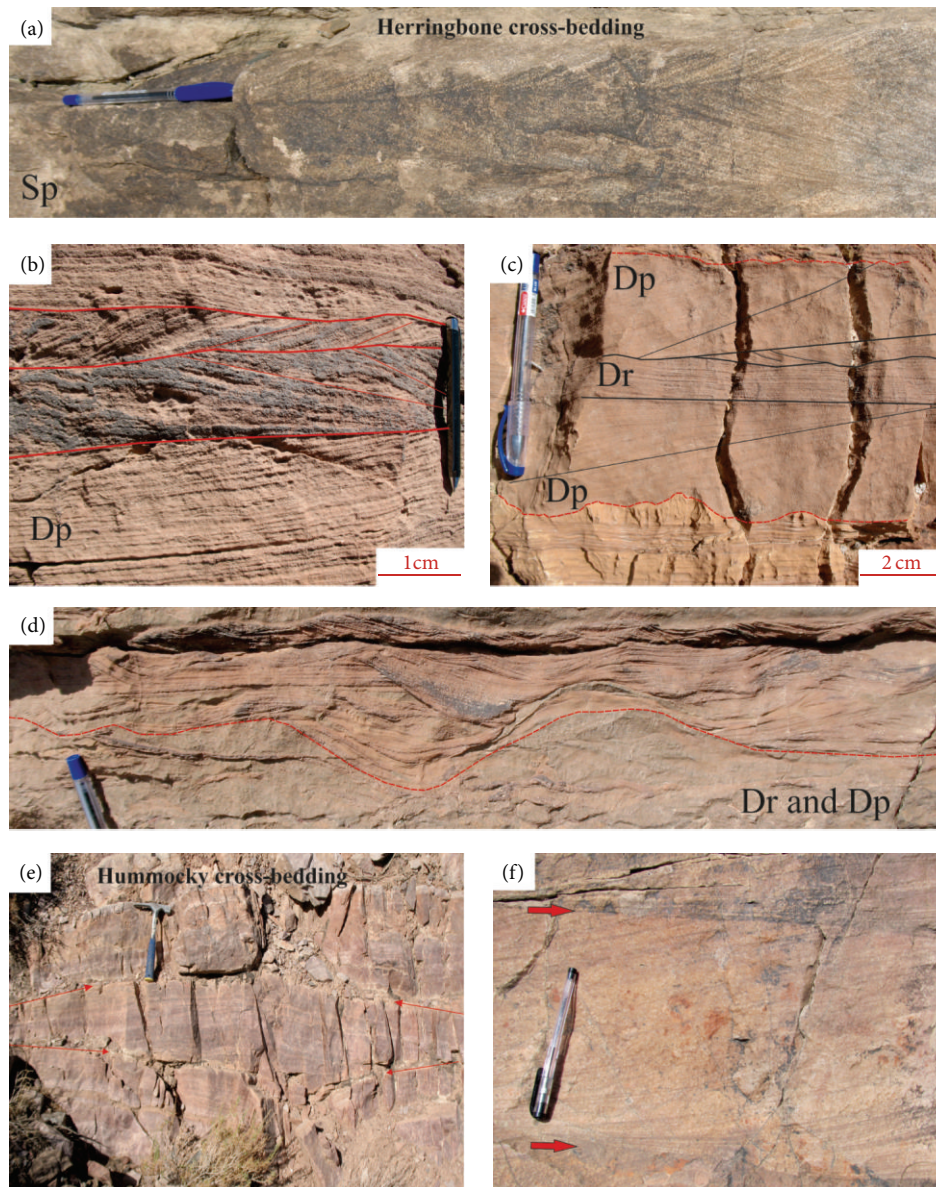


FIGURE 6: Cross-beds in tidalites. (a) Herringbone cross-bedded in Sp lithofacies of Top Quartzite sandstones. (b), (c), and (d) Herringbone, planar, and ripple cross-beds in carbonate tidalites (Deranj Formation). (e) Hummocky cross-beds in sandstone layers in Padeha Formation. (f) Reactivation surfaces (arrows) in the sandstone of Padeha Formation.

(Figure 1), these sections cannot be correlated lithostratigraphically. However, the lithofacies analysis and interpretation of sedimentary environment resulted in identification of tidal facies in the studied sections.

Based on the sedimentological analysis, 17 lithofacies and 4 architectural elements (SB, LA, FE, and EF) were recognized in the Padeha Formation and are classified into sandstone, mudstone, interbedded sandstone-mudstone, carbonate, interbedded sandstone-dolomite, and evaporite lithofacies associations (Tables 1 and 2). It is obvious that the lithofacies distribution in three stratigraphic sections is different. In the type section, the Padeha Formation with 492 m thickness consists of siliciclasts, dolomites, and evaporites with 16 lithofacies (Figure 4). Four lithostratigraphic units were identified

on the basis of detailed field description. These units are dolomite-sandstone (with 48 m thickness comprising D1, Ds, Sr, Sh, Sp, Sr(Fl), and Sr/Fl lithofacies), evaporite-shale (with 194.5 m thickness comprising E1, Efl, Efm, Edl, Sr, Fl(Sr), Sp, and Sh lithofacies), sandstone-dolomite (with 67 m thickness comprising Sp, St, Sr, Sl, Sh, Se, Ds, and D1 lithofacies), and evaporite-shale (with 182.5 m thickness comprising E1, Efl, Efm, Edl, Sr, Fl(Sr), Sp, Sh, and Se lithofacies). These units sequentially reflect subtidal-intertidal, supratidal-sabkha, intertidal, and supratidal-sabkha (Figure 4).

In the Dahane-Kalot section, the Padeha Formation is 320 m thick. Based on the field observations, three lithostratigraphic units were described. The lower unit of the formation consists of a 97 m thick succession of sandstone-dolomite

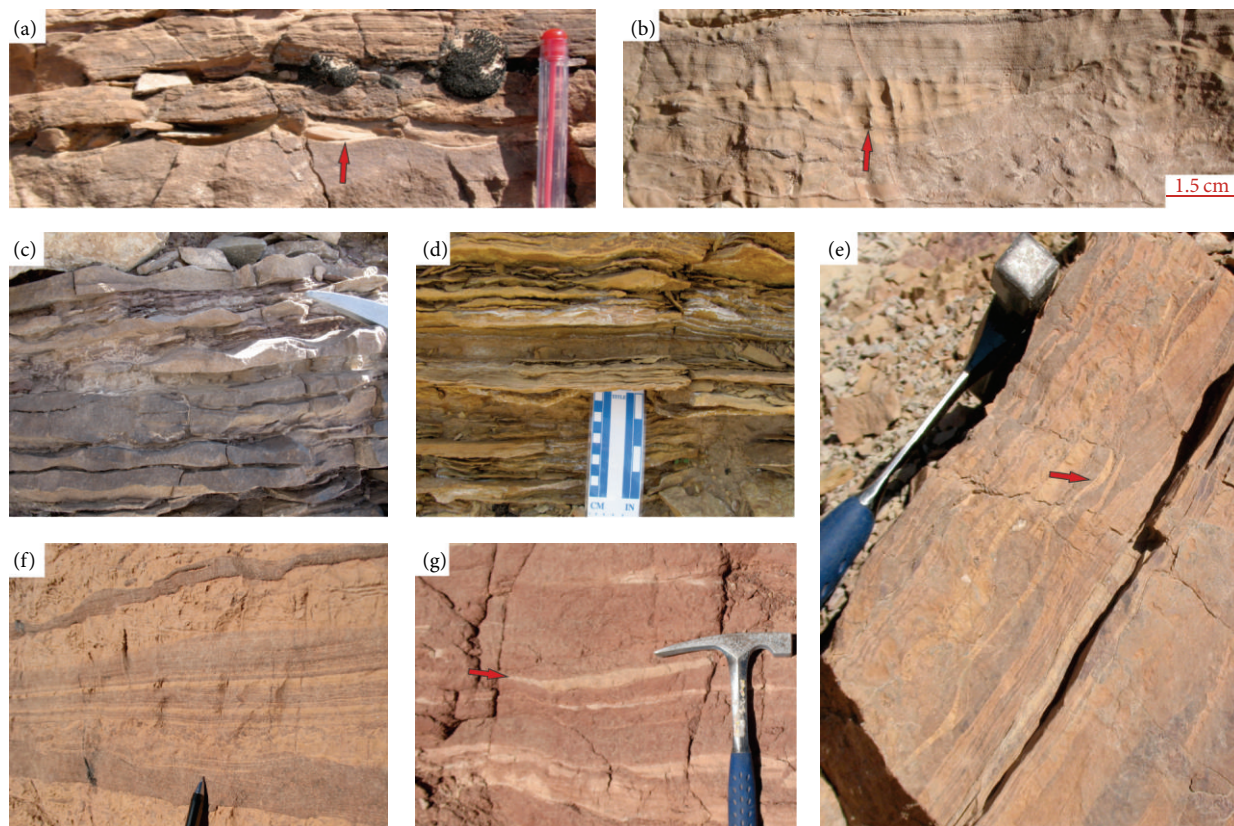


FIGURE 7: Field photos of the heterolithic layers in studied tidalites. (a) Flaser bedding (Sr/Fl) lithofacies) in the Padeha Formation. Arrow indicates a mudstone lens. (b) Flaser bedding (Dr/Dl lithofacies) in the carbonate tidalites (Deranjai Formation). Arrow indicates a dolomudstone lens. (c) Wavy bedding in the Top Quartzite. (d) Wavy bedding in the Padeha Formation. (e) and (f) Interbedded sandstone and dolomudstone (Sr/Dl) in the mixed tidalites of Padeha Formation. (g) Lenticular bedding in the supratidal setting of Padeha Formation. Arrow indicates a sandstone lens.

(Sp, Sr, Sh, Ds, Dl, Sr(Fl), Sr/Fl, Fl(Sr), and Fl lithofacies). The middle unit of the Padeha Formation with 207 m thickness is composed of sandstone-siltstone with Sp, St, Sr, Sl, Sh, Se, Ds, Dl, Sr/Fl, Fl(Sr), and Fl lithofacies. The lithology of the upper unit is dominated by shale-sandstone consisting of a 20 m thick succession of Sh, Se, Sr, Fl(Sr), and Fl lithofacies. The facies analysis revealed that the sediments of the lower and middle units were deposited in intertidal subenvironment, while the identified lithofacies of the upper unit were deposited in supratidal subenvironment.

The Padeha Formation in the Sarashk section, with 297 m thickness, is composed of three lithostratigraphic units. The sandstone of the lower unit (149 m thickness) consist of Sr/Fl, Sr(Fl), Se, Sl, Sh, Sr, St, and Sp lithofacies, deposited in intertidal and partially subtidal subenvironments. The sediments of the middle unit (112 m thickness) are dominated by shale-dolomite and sandstone-dolomite with Fl, Efm, El, Se, St, Sr, Dl, Sr/Dl, and Fl(Sr) lithofacies, indicating supratidal and upper intertidal zones. The upper unit with 36 m thickness is composed of white sandstone. The identified lithofacies include Sl, Sr, St, Sp, Fl, and Sr/Fl. These lithofacies were deposited in an intertidal subenvironment (Figure 4).

Generally, the fining upward cycles and the sedimentary structures (Table 2) including wavy and interference

ripples (Figure 5(c)), herringbone and hummocky cross-beds (Figure 6(e)), reactivation surfaces (Figure 6(f)), flaser, wavy, and lenticular beds (Figures 7(d)–7(g)), mud cracks (Figures 8(e)–8(h)), raindrop imprints (Figure 8(i)), salt casts (Figure 8(j)), enterolithic folding (Figure 8(k)), stromatolitic and tepee structures (Figures 9(h)–9(j)), and bimodal-bipolar paleocurrents are considered as the main diagnostic features in such tidalite systems. The dominant petrofacies in the sandstone lithofacies are quartzarenite with few litharenite. Siltstone and claystone are also the dominant fine-grain petrofacies. Dolomudstone and sandy dolomudstone are the main microfacies present in the dolomite lithofacies. Petrography observations and analysis of microstructures (SEM-EDX methods) within the mudstones and evaporite indicate the presence of gypsum and little anhydrite and clay minerals such as illite, chlorite, and kaolinite in these lithofacies [33].

5. Discussion

The identified tidalites in three depositional systems are compared, based on structural, textural, and architectural elements, through the following sections.

TABLE 3: Comparison of architectural elements and their interpretation in three tidalite systems.

| Architectural element | Code | Lithofacies assemblage | Geometry and relationship | Sedimentary environment |
|-----------------------------|------|-------------------------------------------|---------------------------------------------------------|----------------------------------------------------|
| (I) | | | | |
| Channel deposits | CH | Gcm, Gms, Gt, Sp, St, Sr, Sl, Sh, Se, Fl | Erosional base; wedge shaped (laterally less than 50 m) | Tidal channels in intertidal and subtidal settings |
| Lateral-accretion macroform | LA | Sp, St, Sr, Sl | Erosional base; lense shaped | Meandering (ebb channels), in intertidal setting |
| Sandy bedforms | SB | Sp, Sl, Sh, Sr, Sm, Fl, Sr(Fl), Sr/Fl | Sheet and blanket shaped | Sandy flat in intertidal setting |
| Muddy sets | FF | Fl, Fl(Sr), Sp, Sr | Laminated mudstone with sandstone lenses | Supratidal setting |
| (II) | | | | |
| Channel deposits | CH | Dim, Dp, Dr, Dsd, Dsp, Dl | Erosional base; wedge shaped (70 m up to 100 m) | Tidal channels in intertidal and subtidal settings |
| Carbonate bedforms | CB | Dr, Dsd, Dsp, Dl, Dr/Fl, Flc | Sheet and domal shaped | Intertidal setting |
| (III) | | | | |
| Channel deposits | CH | St, Sp, Sr, Sl, Sh, Se, Ds | Erosional base; wedge shaped (40 to 80 m) | Tidal channels in intertidal and subtidal settings |
| Lateral-accretion macroform | LA | Sp, St, Sr, Sl | Erosional base; lense shaped | Meandering (ebb channels), in intertidal setting |
| Sandy bedforms | SB | Sp, Sl, Sh, Sr, Fl, Sr(Fl), Sr/Fl, Ds, Dl | Sheet and platy shaped | Sandy flat in intertidal setting |
| Muddy sets | FF | Fl, Fl(Sr), Sp, Sr, Sh, Sr/Dl | Mudstone laminated with sandstone lenses | Supratidal setting |
| Evaporate-muddy sets | EF | El, Efl, Efm, Edl | Evaporate layers with laminated mudstone | Upper supratidal and sabkha settings |

(I) Top Quartzite (siliciclastics), (II) Deranjai Formation (carbonates), (III) Padeha Formation (mixed siliciclastic-carbonate).

5.1. Structural Lines of Evidence. Shanmugam [37] classified sedimentary lines of evidence within tidalites into 15 different groups as follows: (1) heterolithic facies, (2) rhythmites of sandstone-shale, (3) thick-thin bundles, (4) alternation of parallel and cross-laminations, (5) climbing ripples, (6) double mud layers (mud couplets), (7) cross-beds with mud drapes, (8) superposed bidirectional cross-bedding, (9) sigmoidal cross-bedding with mud drapes, (10) reactivation surfaces, (11) crinkled laminae, (12) elongate mudstone clasts, (13) flaser beds, (14) wavy bedding, and (15) lenticular bedding. Although the tidal currents were the dominant sedimentary processes controlling the tidalites, other sedimentary processes such as currents were also present. Therefore, tidal environments could exist in coastal plains, estuaries, deltas, or back barrier [32] with wave currents. Such conditions reveal that most of the mentioned sedimentary lines of evidence may also occur, not only in tidal system, but in other environments too.

He et al. [38] suggested that bidirectional cross-laminations or cross-beds, flaser, wavy, and lenticular beds are normally observed in tide deposits. Nevertheless, Mulder et al. [39] believed that these sedimentary structures can be formed by turbidity and contour currents too.

In contrast to the ancient paleoenvironments, in the recent coastal sediments, tidal facies and other sedimentary facies formed by currents can easily be reconstructed and observed. Sedimentary textures and structures of tidalites are

the most important factors in interpretation of tidal deposits. Siliciclastic sediments contain more preserved sedimentary structures than carbonates; therefore, it is easier to identify subenvironments.

The high diversity of ripple marks in the Sr lithofacies indicates the presence of different flow regimes in the environment (Figure 5). Such sedimentary conditions are well represented by the Top Quartzite siliciclasts. In these sediments, the changes from wavy to current ripples with sinusoidal, straight, and complex crests in the short distance reflect dominance of wave currents in a tidal flat environment. These types of ripple marks were rarely recognized within the sediments of the Padeha Formation. Instead, symmetrical ripples with sinusoidal and straight crests were observed (Table 2). In the carbonate sediments of the Deranjai Formation, ripple marks were commonly identified as wavy and climbing ripples (Dr lithofacies). The ripple lithofacies are common in intertidal and partially common in the lower parts of supratidal subenvironments.

Herringbone cross-beds and reactivation surfaces are the other sedimentary structures in the studied tidalites (Figure 6). These structures that were observed in Sp and Dp lithofacies were dominant in an intertidal zone and were formed by the movements of ripple marks and wave-shaped dunes [40]. Analyses of recent tidal cycles [5] reveal that tidal currents are more important in the formation of tidalites than other currents. The dominant current resulted

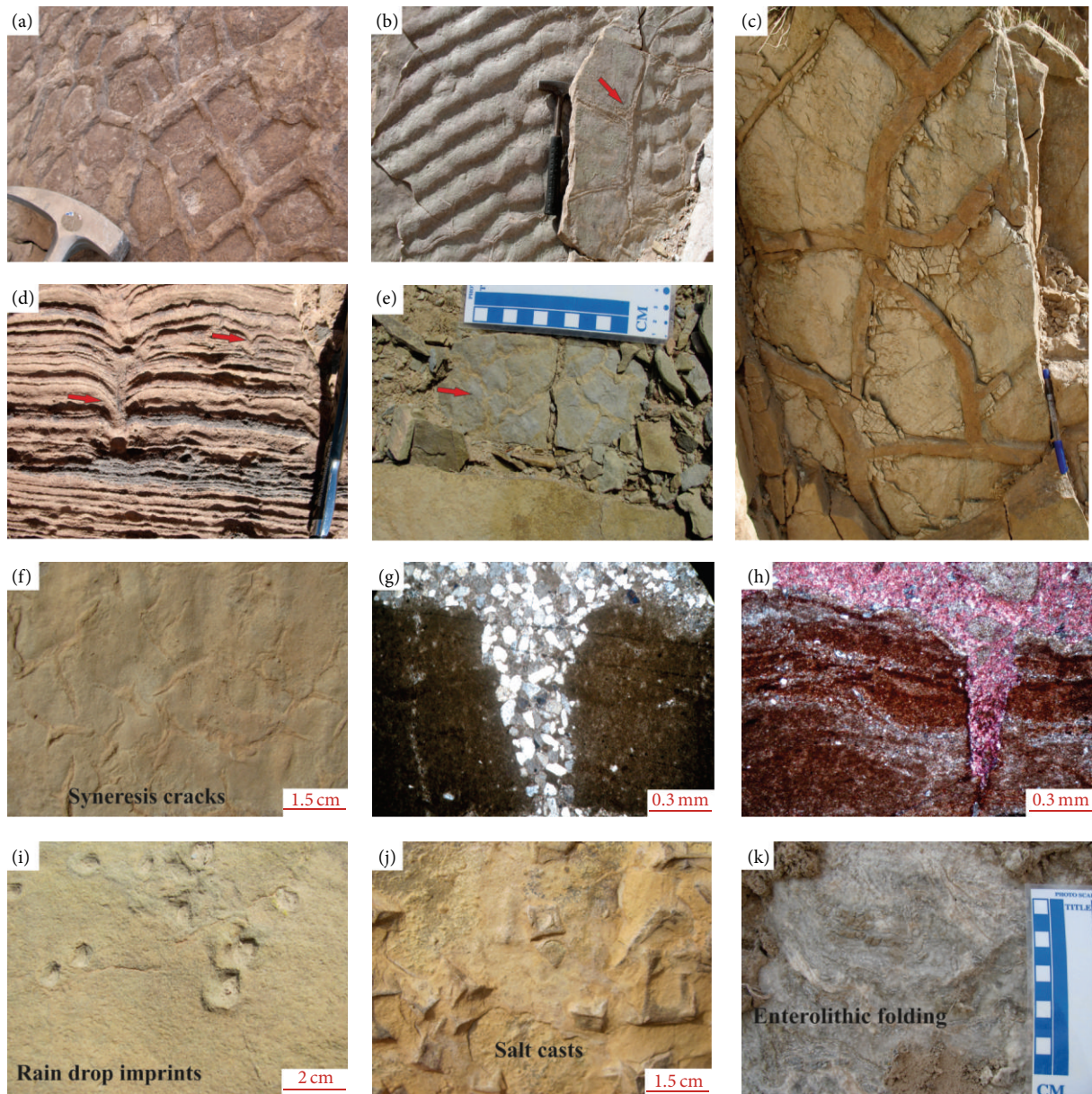


FIGURE 8: Field photos and photomicrographs of some important sedimentary structures in supratidal setting. (a) Polygonal mud cracks in the Top Quartzite. (b) Mud cracks on the rippled sandstones that show upper intertidal conditions. (c) Large-scale mud cracks in the supratidal deposits (Top Quartzite). (d) V-shaped mud cracks in carbonate tidalites (Deranj Formation). (e) Shrinkage and polygonal mud cracks in supratidal setting of the Padeha Formation. (f) Syneresis cracks in the Padeha Formation. (g) V-shaped cracks in mudstone petrofacies (Padeha Formation). (h) V-shaped cracks in dolomudstone microfacies (Padeha formation). (i) Raindrop imprints in the muddy sediments of the Padeha Formation. (j) Salt casts or halite casts in the Padeha Formation. (k), Enterolithic folding in the evaporite deposits (Padeha Formation).

in formation of wavy bedforms and subsequent formation of cross-beds. The current from the opposite direction was lower in energy and therefore it could not lead to formation of cross-beds in an opposite direction. It only eroded the sediments from the ripple surface. This process could result in formation of tidal bundles and cross-beds separated by mud drapes. The occurrence of herringbone cross-beds in sandstone lithofacies as well as mud drapes in the upper parts of fining upward cycles reflects deposition of sediments in

different depth and tidal current energies in an intertidal subenvironment [2, 41, 42].

The flaser, wavy, and lenticular beds (Sr/Fl lithofacies association) in heterolithic layers are also the other typical sedimentary structures in tidal flat environments (Figure 7). These structures are more abundant in siliciclastic systems. Such lithofacies resulted from alternative changes in the environmental energy. Based on the energy variations, sandstone-mudstone and sandstone-carbonate lithofacies

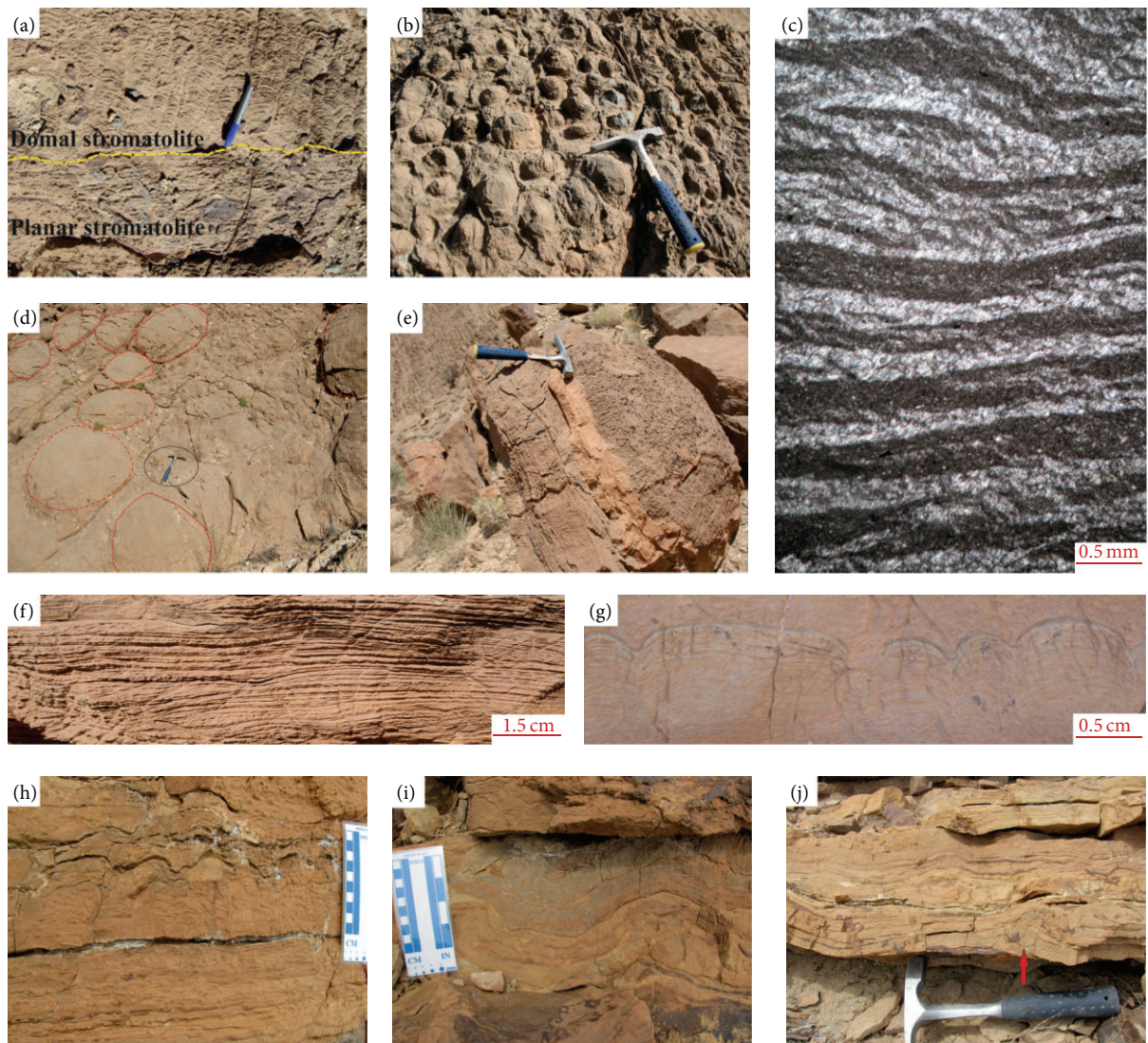


FIGURE 9: Field photos and photomicrographs of stromatolite and associated sedimentary structures in the carbonate tidalites. (a) Cross section of planar and domal stromatolites in the Deranj Formation. (b) Domal stromatolite (small scale) in the Deranj Formation. (c) Boundstone microfacies (stromatolitic) in the Deranj Formation. (d) Large-scale domal stromatolite. These structures are made up of small-scale stromatolites community. (e) Field photo shows that domal stromatolites are often the last layers of channel deposits. (f) Close-up view of planar stromatolite in the Deranj Formation. (g) Cross section of domal stromatolite in the Deranj Formation (close-up view). (h) Photo of stromatolite structures in the Padeha Formation. (i) Tepee structures in the Padeha Formation (without crest fracturing). (j) Tepee structures associated with stromatolite in the Padeha Formation (with crest fracturing (arrow)).

were deposited as heterolithic rhythmites. The heterolithic laminae, which occur in tidalites, are known as doublets or couplets [43]. According to Archer and Greb [44], these beds are often formed during semi- and diurnal tidal currents due to changes in tidalite periods. Based on the field analysis of the siliciclasts of the Padeha Formation and the Top Quartzite succession, three Sr(Fl), Sr/Fl, and Fl(Sr) lithofacies were identified. An increase of energy in the environment (deposition of sandstone lithofacies) led to deposition of Sr lithofacies with several ripples morphologies, whereas, fine-grained mudstone (Fl lithofacies) precipitated in the trough point of ripples during the decrease of energy. Following the deposition of the mudstones, the environmental energy

gradually increased. The alternative changes in the energy level and the elapse time condition result in deposition of interbedded lithofacies comprising flaser, wavy, and lenticular beddings [40, 43]. Within the interbedded sandstone-mudstone, Sr/Fl with wavy beds is the most abundant interbedded lithofacies observed in the Padeha Formation and the Top Quartzite succession. The thickness of each set ranges from 8 cm to 3 m. This lithofacies association is very dominant in tidal flat [2, 4, 40, 45, 46]. Additionally, Sr/Dl lithofacies were identified in the supratidal deposits of the Padeha Formation reflecting interaction of physical and chemical processes in the sedimentary environment (Figure 7). This led to an input of siliciclastic and formation of

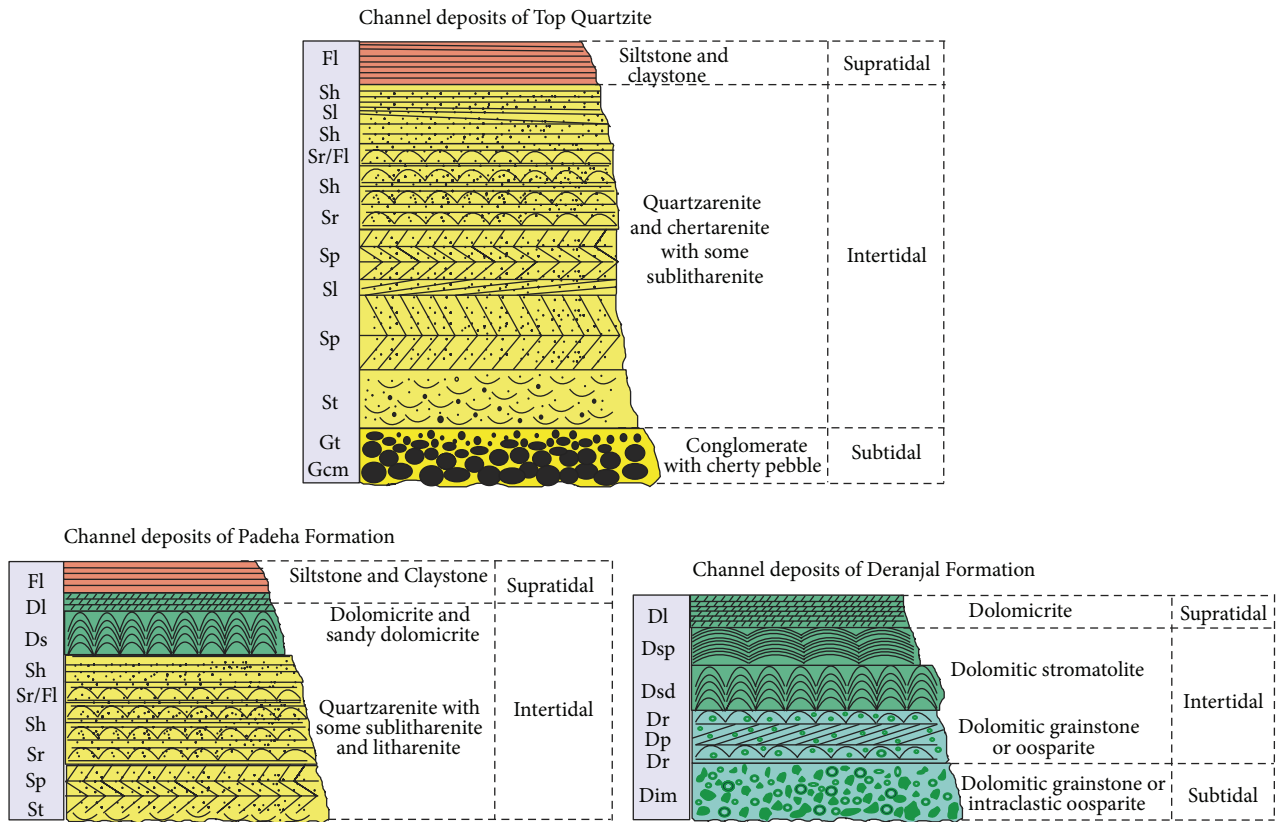


FIGURE 10: Schematic vertical columns and comparison of channel deposits (CH element) in three tidalite systems.

sandstone lenses within the dolomudstone microfacies. The flaser beddings were also recognized within the carbonate deposits of the Deranj Formation and are composed of Dr/Dl lithofacies.

Mud cracks and raindrop imprints are the two major sedimentary structures found in tidal flat deposits and are well preserved within the siliciclasts (Figure 8). In the siliciclastic sediments of the Padeha Formation and the Top Quartzite succession, the mud cracks appeared as polygons on the surfaces of fine-grained sandstones and siltstones. Syneresis cracks were also observed in these sediments of the Padeha Formation resulting from salinity changes [47]. Additionally, some V-shaped mud cracks were identified in the carbonates of the Deranj Formation (Figure 8(d)). Mud cracks are commonly related to the supratidal and upper intertidal zones. Stromatolites and stromatolitic structures are two of the most abundant sedimentary structures within the carbonate settings (Figure 9). The stromatolites occur in different sizes and morphologies (domal (Dsd) and planar (Dsp)) within the carbonate layers of the Deranj Formation. Such sedimentary structures are abundant in the tidal flat deposits, particularly in the intertidal zone [5, 11].

In the carbonate deposits, tepee structures are also observable. Tepee structures are common in tidalites and are formed as a result of desiccation, cementation and crystal growth, thermal expansion, and contraction of partially lithified sediment in arid tidal flat or high-energy shallow subtidal sediments [11, 48]. Due to lithology changes, the tepee

structures are more dominant in the mixed siliciclastic-carbonate sediments.

5.2. Textural Lines of Evidence. In addition to sedimentary structures, textural feature is also one of the main factors in identification of tidal flat sediments. The texture of siliciclastic rocks consists of size, shape, and fabric of the grains. In the studied siliciclastic deposits, grain size ranges from pebble to silt size. Well-rounded pebbles were only observed within the sediments of the Top Quartzite succession reflecting dominance of wave currents and tidal currents during transportation and sedimentation. Recent tidal deposits have high compositional and textural maturity similar to the studied sandstones.

The most abundant petrofacies within the Top Quartzite and Padeha Formation are mature to supermature quartzarenite with a few chertarenite. The textural inversion and bimodality in some petrofacies reflect the effects of sedimentary currents (e.g., waves and wind) in the tidal flat zone. The importance of textural features is also obvious in the carbonate rocks. In addition to parameters such as the roundness and sorting of carbonate grains, the types of grains are also the other important factors in identification of carbonate tidalites.

Ooids, intraclasts, and peloids are the most common grains in the carbonate deposits of the Deranj Formation. The matrix or the cement is also considered as a useful factor

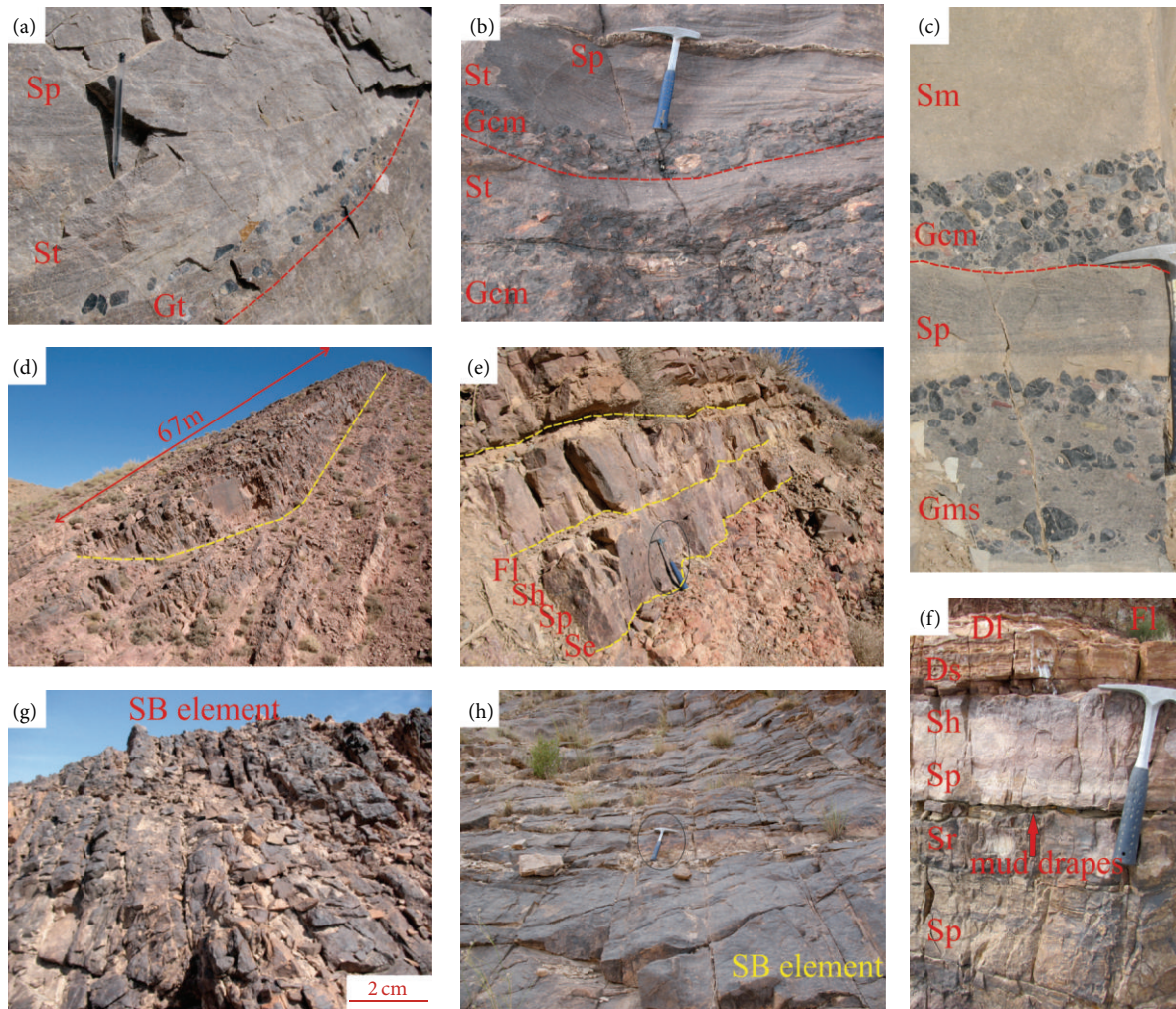


FIGURE 11: Filed photos show characteristics of channel deposits in the siliciclastic and mixed tidalites. (a), (b), and (c) Photos show channel deposits in the Top Quartzite and their lithofacies assemblage. Red lines separate fining upward cycles. (d) Photo shows vertical and lateral (67 m) variations in channel deposits in the Padeha Formation. (e) lateral accretion (LA element) in meandering (ebb channels) in the Padeha Formation. (f) Close-up view of a fining and shallowing upward cycle in the mixed tidalites (Padeha Formation). (g) Photo of sandy bedforms element (SB) in the Padeha Formation. (h) Photo of sandy bedforms element (SB) in the Top Quartzite sandstones.

in interpretation of microfacies (e.g., [7, 28]). The microfacies in Deranj Formation are dolomudstone, dolomitic mudstone, dolomitic peloidal packstone, dolomitic ooidal-intraclastic wackstone-packstone, dolomitic ooidal grainstone, and dolomitic ooidal-intraclast grainstone (Tables 1 and 2).

Generally, dolomitic mudstone with fenestral fabric, dolomitic peloidal wackstone-packstone, ooidal-intraclastic packstone, and domal stromatolitic boundstones indicate low-energy conditions of subtidal lagoon (e.g., [11, 49, 50]). In addition, ooidal or intraclastic grainstones and stromatolitic boundstones (often planar shaped) are formed in high-energy conditions, especially tidal channels in intertidal and shallow subtidal settings. Vertical and lateral variations of the lithofacies led to recognition of several architectural elements and paleoenvironmental reconstruction. Other sedimentary textures observed in the studied microfacies are fenestral fabrics, calcite pseudomorphs (only in the Padeha Formation), and

V-shaped mud cracks within the dolomudstone lithofacies (Table 2). The presence of such textures indicates deposition of the sediments in the upper intertidal and supratidal zones (e.g., [11, 49–52]).

5.3. Architectural Elements. The identified architectural elements within tidal deposition systems are CH, LA, SB, CB, FF, and EF (Table 3); that will be discussed next.

5.3.1. Channel Deposits (CH). The CH is one of the major elements that are common in three tidal systems. Tidal channels contain a wide range of bedforms with different sizes, forming with bidirectional currents in shallow marine environments to sandy barriers [53]. Tidal channels are usually present in intertidal and subtidal zone and commonly have dendritic network. Several factors, such as physical and hydrodynamic process, control the morphology and

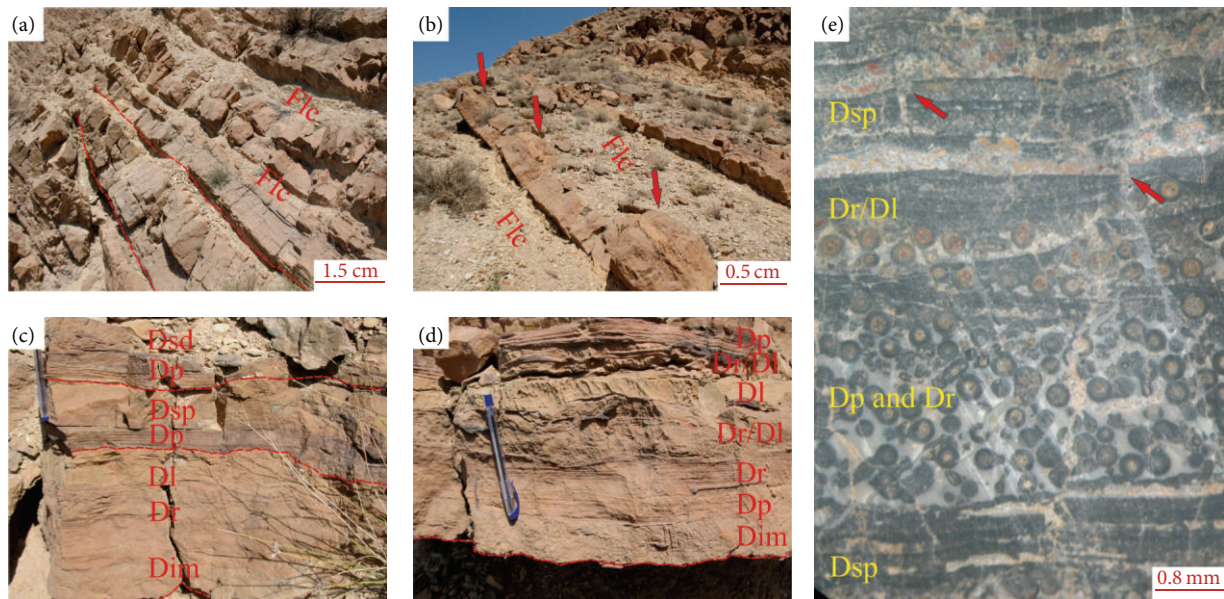


FIGURE 12: Field photos and photomicrograph show the characteristics of channel deposits in the carbonate tidalites (Deranjai Formation). (a) Tidal channel deposits between subtidal lagoon deposits (Flc lithofacies). (b) Domal stromatolites on the channel deposits (arrows). (c) and (d) Close-up view of lithofacies assemblage of channel deposits in the carbonate tidalites. (e) Photomicrograph of tidal channel deposits. Dolomitic ooid grainstone is common at the base of channel deposits and generally changes to, stromatolite toward the top. Arrows show v-shape cracks in stromatolite.

distribution of tidal channels (e.g., [54]). The channel-filling sediments are commonly showing shallowing upward cycles. Abundance of bidirectional structure such as planar and herringbone cross-beds and ripple marks as well as the presence of channel lag (at the base) along with thin sandstone layers and the lines of evidence of exposure (e.g., mud cracks and raindrop imprints) in an upward direction reflects tidal channel deposits [42, 46, 53].

In the siliciclastic depositional systems, fining upward of sediments shows either a decrease of energy or a shallowing upward trend in the sedimentary environment. Within the Top Quartzite succession, the basal parts of the channel deposits are composed of chert pebbles or coarse-grained sandstones changing into fine-grained sandstone or siltstone in an upward direction (Figures 10(a) and 11(a)–11(c)). In the shallowing upward cycles of siliciclastic systems, from the base to the top, a sedimentary succession typically consists of the following lithofacies: (Gcm, Gt, Gp)-(St, Sp)-(Sl, Sh, Sr)-(Sr(Fl), Sr/Fl, and Fl(Sr))-(Fl). In the Top Quartzite siliciclasts, this succession was deposited either as an incomplete or a complete (Figures 11(a)–11(c)) and extends laterally about 10–30 m with 3 to 10 m in thickness.

In the channel deposits of the mixed siliciclastic-carbonate succession of the Padeha Formation, the base part is erosional and is composed of medium to coarse-grained sandstones that subsequently change into dolomites and stromatolitic limestone at the top (Figures 10(b) and 11(d)–11(f)). The channel deposits of the Padeha Formation are 1–5 m thick with lateral extension of 40–70 m. The trend which is typically representative of shallowing upward cycles in

the channel sediments of the Padeha Formation is as follows: (St, Sp)-(Sl, Sh, Sr)-(Sr(Fl), Sr/Fl, Fl(Sr))-(Fl, Ds, Dl).

The thickness of the element in the tidal carbonate system of the Deranjai Formation is less than in other depositional systems. Typically, the basal parts of the deposits are mostly composed of dolomitic ooidal-intraclast grainstone microfacies with erosional base that changes to dolomitic ooidal packstone and grainstone with ripple lamination toward the top (Figures 10(c) and 12). Following this shallowing upward trend, the dolomitic stromatolitic boundstone with a few dolomudstone beds was deposited. These lithofacies are mainly intercalated with alternations of subtidal lagoon carbonate mudstones (marls). The CH element in these deposits typically consists of (Dim)-(Dr, Dp)-(Dsd, Dsp, Dr/Dl)-(Dl) lithofacies with vertical thickness of 1–3 m and lateral extension of 30–100 m. The Dim lithofacies is composed of rounded, poorly sorted limestone clasts that are deposited by debris flows in tidal or storm channels in tidal flats. These lithofacies are common on Cambrian and Ordovician carbonate platforms (e.g., [55, 56]).

The comparison of the CH element in these three depositional systems shows that the channel deposits in the siliciclastic systems have the least lateral extension with the maximum vertical thickness. Hughes [53] discussed that tidal channels can exist in different depths and hydrodynamic conditions that directly control the CH element. The channels in the deeper environments are more extended and preserved than the shallow channels. The facies and environmental analysis of the Deranjai Formation indicate that such channels were mostly extended in barrier and subtidal lagoon and

therefore, the depth of the environment could control the distribution of channel element in the sediments than the deposits of the Top Quartzite and the Padeha Formation.

5.3.2. Lateral-Accretion Bedforms (LA). This element is considered as a part of channel deposits formed by lateral accretion of meandering channels (e.g., [40, 57]). Sudden movements of channels result in the establishment of fining and shallowing upward cycles with more limited lateral movements than CH element (Figure 11(e)). The LA element is common in the siliciclastic tidalites and none was identified in the carbonate tidalites.

5.3.3. Sandy Bedforms (SB). The SB element is linear in plane view and asymmetrical in cross section. They are parallel to the main flow of tidal currents. Sand on these sedimentary bodies ranges in size from very fine to very coarse grained depending on availability, and sorting in the bedforms developed on the sand bodies includes wavy and current ripples and dune [4]. The Sp, Sh, Sm, and Sr lithofacies are the dominant constituents of this type of element (Table 3). The Gp and Gt lithofacies are also the other types of lithofacies in the siliciclastic sediments of the Top Quartzite. In the mixed siliciclastic-carbonate system (the Padeha Formation), thin layers of D1 and Ds lithofacies and also sandstone lithofacies are composed of the SB element (Figures 11(g) and 11(h)). The SB element is not observed in the carbonate tidalites. According to the identified lithofacies, the SB element is often formed in tidal flats or intertidal zone due to high sedimentation rate of sand-sized grains. Intertidal sand body systems have been accumulated in areas with relatively strong bottom tidal current velocities, subjecting the seabed with a high rate of sand transport by bedload processes of deposition [4].

5.3.4. Carbonate Bedforms (CB). In the carbonate deposits of the Deranj Formation consisting mainly of boundstone and dolomudstone microfacies, Ds and D1 are the major constituents of this type of element. However, thin layers of mudstone were deposited between the lithofacies as mud drapes. Based on the sedimentation rate of the carbonate materials in the mixed siliciclastic-carbonate depositional system, the CB element could be present. Scattered CB element was identified in the lower part of the Padeha Formation at the type section. The identified lithofacies associations in the CB revealed that this element was formed in an intertidal and the lower parts of a supratidal subenvironment.

5.3.5. Fine-Grained Beds (FF). This element is composed of fine-grained mudstones with dominant Fl as well as Sr and Sp lithofacies. The structural characteristics and the stratigraphic position of the facies associations reflect deposition of these lithofacies in a low-energy supratidal zone. The FF element was clearly recognized within the Top Quartzite and the Padeha Formation. The sandstone lithofacies were mainly deposited during the flood and input of flooding channels to a supratidal subenvironment (e.g., [49]). The flooding channel deposits are 20 cm to 1 m thick and have a limited lateral

extension. Although the FF element can also be formed in carbonate tidal environments (e.g., [11]), no traces of such element were found in the carbonates of the Deranj Formation.

5.3.6. Evaporite-Mud Rocks Beds (EF). The EF element consists of an assemblage of evaporite lithofacies. Generally, evaporites can be formed in all three depositional systems but are only recognized in the Padeha Formation. An arid climate and an idealized coastal morphology, to deposition of evaporite in sabkha or salina. Such environmental conditions were prevailing during the formation of the mixed siliciclastic-carbonate tidalites of the Padeha Formation, and El, Efl, Efm, and Edl lithofacies were formed the EF framework in a coastal sabkhas. Sedimentary structures such as mud cracks, raindrop imprints, and wavy ripples as well as the presence of primary fine-grained dolomites show that the facies associations were formed in a continental-coastal environment (subaerial precipitation). In this model, evaporite deposits are formed in the sediments above the tidal flat zones or sabkha environment. Low energy in this area caused deposition of fine-grained clay-sized deposits. If conditions are ready for precipitation of evaporite deposits, gypsum and anhydrite are precipitated from the pore waters in vadose and upper phreatic zones with respect to capillary properties between fine-grained sediment (mudstone) [47, 58].

The El, Efm, and Efl lithofacies within the Padeha Formation were deposited in such conditions. According to the classification of sabkhas [59, 60] and the lithofacies characteristics, the evaporite facies of the Padeha Formation were formed in marine or coastal sabkhas. These sabkhas were present either in dry or arid climates between land and sea, but the source of brine is often from the sea. Thus, the lithofacies of these environments consist of evaporite deposits, particularly gypsum and in some cases anhydrite with evaporitic dolomite and siliciclastic facies [47, 61]. Depositions of primary dolomite are carried out prior to or simultaneously with the process of forming evaporite minerals. Dolomites were formed when the ratio of Mg/Ca was rising in the environment. Deposition of gypsum caused the concentration of calcium ions to decrease, therefore, providing conditions for the formation and deposition of dolomite. This process is the most important factor in formation of Edl facies in the studied settings. These lithofacies have a wide stratigraphic distribution in the Padeha Formation at the type section. Efm and El are the only lithofacies identified in the Sarashk section. The limited extension of evaporite facies in the Kerman area reflects sedimentation in a salina flat.

6. Conclusions

Based on facies analysis and comparison of tidalites in siliciclastic, carbonate, and mixed siliciclastic-carbonate systems in the Cambrian and Devonian of central Iran, the following results have been obtained.

(1) The Lower-Middle Cambrian Top Quartzite is a representative of siliciclastic tidal system. It consists of conglomerate (Gt, Gms, and Gcm), sandstone (Sp, St, Sh, Sl, Sr, Sm, and Se), interbedded sandstone-mudstone (Sr(Fl), Sr/Fl, and

Fl(Sr)), and mudstone (Fl) lithofacies. The lithofacies associations were formed in three CH, SB, and FF (CH) elements.

(2) The Upper Cambrian carbonate deposits (equivalent to the Deranj Formation) are interpreted as carbonate tidalites. Six lithofacies (Dim, Dp, Dr, Ds, Dl, and Dr/Dl) were identified in these deposits. The lithofacies consist mainly of ooidal-interclastic grainstone and packstone, boundstone and dolomudstone. The sediments were dolomitized with well-preserved original texture. The sedimentological analysis led to recognition of two CH and CB elements that were deposited in intertidal and subtidal lagoon. The supratidal lithofacies have a limited stratigraphic extension.

(3) Tidalites from a mixed siliciclastic-carbonate system were described from the siliciclasts, carbonates, and evaporites of the Padeha Formation (Lower-Middle Devonian). 17 lithofacies were recognized in these deposits and are classified into six facies associations. The lithofacies include sandstone (Sp, St, Sh, Sl, Sr, and Se), mudstone (Fl), interbedded sandstone-mudstone (Sr(Fl), Sr/Fl, and Fl(Sr)), carbonate (Ds and Sl), interbedded sandstone-dolomite (Sr/Dl), and evaporite (El, Efm, Efl, and Edl). The lithofacies associations are subdivided into five CH, LA, SB, FF, and EF elements that were deposited in subtidal-intertidal, intertidal, supratidal, and sabkha environments, respectively.

(4) The lithofacies analysis of the three studied tidalites reveals that the mixed siliciclastic-carbonate systems contain the most diverse sedimentary structures. Instead, in the siliciclastic depositional systems, the sedimentary structures are present in larger scales. The most significant texture and sedimentary structures of the tidalites, which are the same in the three depositional systems but different in abundance, include wavy, current, and interference ripples, herringbone cross-beds, reactivation surfaces, flaser, wavy, and lenticular bedding, mud cracks, and raindrop imprints, but are well preserved within the siliciclastic sediments. In the carbonate tidalites stromatolitic and tepee structures, small-scale V-shaped mud cracks, fenestral fabrics, and pseudomorph calcite are more abundant.

(5) The architectural elements revealed that the channel element (CH) is the most important element in the tidalites and is observed in the shallowing upward cycles. In the siliciclastic sediments, the channel element is composed of fining upward (conglomerate-sandstone to sandstone-mudstone) cycles. In the carbonate tidalites, this element is representative of vertical changes of dolomitic ooidal and interclastic grainstones to packstone and stromatolitic boundstones. Finally, the CH element in siliciclastic tidalites has the greatest vertical thickness and the least lateral extension than in other systems. Instead, channel deposits in carbonate tidalites have the least vertical thickness and the greatest lateral extension.

Acknowledgments

This work is a part of a PhD thesis of Hamed Zand-Moghadam, which is supported by the Department of Geology at Ferdowsi University of Mashhad, Iran. The authors would like to acknowledge their logistical and financial

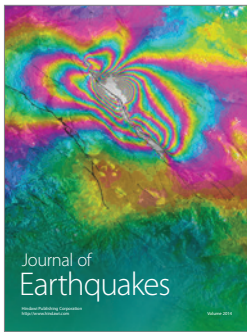
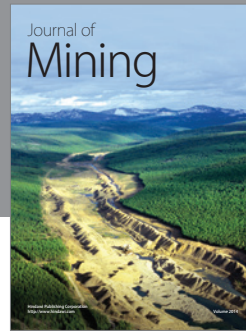
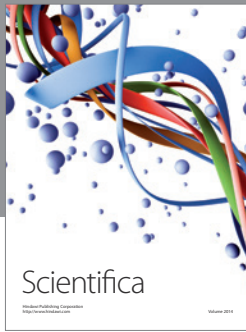
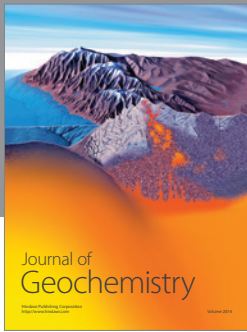
support. They are grateful to Dr. Amir Hossin Rahiminejad for editing the paper and Dr. Javad Hasani, Dr. Ahmad Raoufian, and Dr. Ali Aghaei for their contributions to this study, especially during fieldwork.

References

- [1] A. D. Miall, *The Geology of Fluvial Deposits: Sedimentary Facies, Basin Analysis and Petroleum Geology*, Springer, New York, NY, USA, 2006.
- [2] G. D. Klein, "A sedimentary model for determining paleo tidal range," *Geological Society of America Bulletin*, vol. 82, pp. 2585–2592, 1971.
- [3] G. D. Klein, "Determination of paleotidal range in clastic sedimentary rocks," in *Proceedings of the 24th International Geological Congress*, no. 6, pp. 397–405, 1972.
- [4] G. D. Klein, "Clastic tidalites—a partial retrospective view," in *Tidalites: Processes and Products*, C. R. Alexander, R. A. Davis V, and J. Henry, Eds., no. 81, pp. 5–14, SEPM.
- [5] R. A. Davis, "Tidal signatures and their preservation potential in stratigraphic sequence," in *Principles of Tidal Sedimentology*, R. A. Davis and R. W. Dalrymple, Eds., pp. 35–55, Springer, Heidelberg, Germany, 2012.
- [6] V. P. Wright, "Peritidal carbonate facies models: a review," *Geological Journal*, vol. 19, no. 4, pp. 309–325, 1984.
- [7] E. Flügel, *Microfacies of Carbonate Rocks, Analysis, Interpretation and Application*, Springer, Berlin, Germany, 2010.
- [8] B. R. Pratt, "Peritidal carbonates," in *Facies Models*, N. P. James and R. W. Dalrymple, Eds., GEO text 4, pp. 401–420, Geological Association of Canada, St. John's, Canada, 2010.
- [9] J. F. Read, "Carbonate platform facies models," *American Association of Petroleum Geologists Bulletin*, vol. 66, pp. 860–879, 1985.
- [10] R. V. Demicco and L. A. Hardie, "Sedimentary structures and Lower diagenetic features of shallow marine carbonates," in *Atlas Series 1*, Society of Sedimentary Geology, Tulsa, Okla, USA, 1994.
- [11] Y. Lasemi, D. Jahani, H. Amin-Rasouli, and Z. Lasemi, "Ancient carbonate tidalites," in *Principles of Tidal Sedimentology*, R. A. Davis and R. W. Dalrymple, Eds., pp. 567–607, Springer, Heidelberg, Germany, 2012.
- [12] M. Takin, "Iranian geology and continental drift in the Middle East," *Nature*, vol. 235, no. 5334, pp. 147–150, 1972.
- [13] A. M. C. Şengör, "A new model for the late Palaeozoic-Mesozoic tectonic evolution of Iran and implications for Oman," *Geological Society Special Publication*, vol. 49, no. 1, pp. 797–831, 1990.
- [14] J. Stocklin, "Structural history and tectonics of Iran: a review," *American Association of Petroleum Geologists Bulletin*, vol. 52, no. 7, pp. 1229–1258, 1968.
- [15] R. Huckriede, M. Kursten, and H. Venzlaff, "Zur Geologie. des Gebietes zwischen Kerman und Saghand (Iran)," *Beiheft Zum Geologischen Jahrbuch*, no. 51, 1962.
- [16] M. Alavi, "Sedimentary and structural characteristics of the Paleo-Tethys remnants in northeastern Iran," *Geological Society of America Bulletin*, vol. 103, no. 8, pp. 983–992, 1991.
- [17] M. Wilmsen, F. T. Fürsich, K. Seyed-Emami, M. R. Majidifard, and M. Zamani-Pedram, "Facies analysis of a large-scale Jurassic shelf-lagoon: the Kamar-e-Mehdi formation of east-central Iran," *Facies*, vol. 56, no. 1, pp. 59–87, 2010.

- [18] M. I. Husseini, "Tectonic and deposition model of Late Precambrian-Cambrian Arabian and adjoining plates," *American Association of Petroleum Geologists Bulletin*, vol. 73, no. 9, pp. 1117–1131, 1989.
- [19] A. Aghanabati, *Geology of Iran*, Geological Survey of Iran, 2004.
- [20] M. I. Husseini, "Tectonic and depositional model of the Arabian and adjoining plates during the Silurian-Devonian," *American Association of Petroleum Geologists Bulletin*, vol. 75, no. 1, pp. 108–120, 1991.
- [21] A. S. Al-Sharhan and A. E. M. Nairn, *Sedimentary Basins and Petroleum Geology of the Middle East*, Elsevier, Amsterdam, The Netherlands, 1997.
- [22] J. Golonka, "Phanerozoic paleoenvironment and paleolithofacies Maps. Late Paleozoic," *Geologia*, vol. 33, no. 2, pp. 145–209, 2007.
- [23] J. Golonka, "Phanerozoic Paleoenvironment and Paleolithofacies Maps. Early Paleozoic," *Geologia*, vol. 35, no. 4, pp. 145–209, 2009.
- [24] Y. Lasemi, "Facies Analysis, Depositional Environments and Sequence Stratigraphy of the Upper Pre-Cambrian and Paleozoic Rocks of Iran," *Geological Survey of Iran*, 2001 (Persian).
- [25] J. Wendt, B. Kaufmann, Z. Belka, N. Farsan, and A. K. Bavandpur, "Devonian/Lower Carboniferous stratigraphy, facies patterns and palaeogeography of Iran Part II. Northern and central Iran," *Acta Geologica Polonica*, vol. 55, no. 1, pp. 31–97, 2005.
- [26] J. A. D. Dickson, "Carbonate identification and genesis as revealed by staining," *Journal of Sedimentary Petrology*, vol. 36, pp. 441–505, 1996.
- [27] R. L. Folk, *Petrology of Sedimentary Rocks*, Hemphill, Austin, Tex, USA, 1980.
- [28] R. J. Dunham, "Classification of carbonate rocks according to depositional texture," in *Classification of Carbonate Rocks*, W. H. Ham, Ed., pp. 108–121, American Association of Petroleum Geologists, 1962.
- [29] R. Moussavi-Harami, A. Mahboubi, A. Kheradmand, and H. Zand-Moghadam, "Lithofacies analysis and fining upward cycles of siliciclastic sediments of Dahu Formation (Lower Cambrian) in the East and Southeast of Zarand, NW Kerman," *Iranian Journal of Geology*, vol. 2, pp. 71–85, 2008 (Persian).
- [30] H. Zand-Moghadam, R. Moussavi-Harami, and A. Mahboubi, "Tidal sediments analysis of Top Quartzite in East of Zarand in Kerman area," *Journal of Stratigraphy and Sedimentology Reserches the University of Isfahan*, no. 37, pp. 1–18, 2009 (Persian).
- [31] H. Bavi, R. Moussavi-Harami, A. Mahboubi, and M. Nadjafi, "Comparison of facies associations of Upper Cambrian deposits in the south of Central Iran and central Alborz," in *Proceedings of the 6th National Geological Conference of Payame Noor University, Kerman-Iran*, pp. 622–627, 2012.
- [32] D. Fan, "Open-coast tidal flat," in *Principles of Tidal Sedimentology*, R. A. Davis and R. W. Dalrymple, Eds., pp. 187–229, Springer, Heidelberg, Germany, 2012.
- [33] H. Zand-Moghadam, R. Moussavi-Harami, and A. Mahboubi, "Facies analysis of tidal flat-sabkha deposits of Padeha Formation in Ozbak-Kuh Mountains (type section)," in *Proceedings of the 16th Symposium of Geological Society of Iran*, Shiraz University, Iran, 2012.
- [34] A. Ruttner, M. H. Nabavi, and J. Hajian, "Geology of Shirgesht area (Tabas area, East Iran)," Tech. Rep. 4, Geological Society of Iran, 1968.
- [35] M. Alavi-Naini, "Paleozoic stratigraphy of Iran," *Geology Survey of Iran, Treatise on the Geology of Iran*, no. 5, 1993.
- [36] J. Wendt, B. Kaufmann, Z. Belka, N. Farsan, and A. K. Bavandpur, "Devonian/Lower Carboniferous stratigraphy, facies patterns and palaeogeography of Iran. Part I. Southeastern Iran," *Acta Geologica Polonica*, vol. 52, no. 2, pp. 129–168, 2002.
- [37] G. Shanmugam, "Deep-marine tidal bottom currents and their reworked sands in modern and ancient submarine canyons," *Marine and Petroleum Geology*, vol. 20, no. 5, pp. 471–491, 2003.
- [38] Y. He, Z. Gao, J. Luo, S. Luo, and X. Liu, "Characteristics of internal-wave and internal-tide deposits and their hydrocarbon potential," *Petroleum Science*, vol. 5, no. 1, pp. 37–44, 2008.
- [39] T. Mulder, S. Migeon, B. Savoye, and J.-C. Faugères, "Inversely graded turbidite sequences in the deep Mediterranean: a record of deposits from flood-generated turbidity currents?" *Geo-Marine Letters*, vol. 21, no. 2, pp. 86–93, 2001.
- [40] K. Strand, "Sequence stratigraphy of the siliciclastic East Puolanka Group, the Palaeoproterozoic Kainuu Belt, Finland," *Sedimentary Geology*, vol. 176, no. 1-2, pp. 149–166, 2005.
- [41] A. Folkestad and N. Satur, "Regressive and transgressive cycles in a rift-basin: depositional model and sedimentary partitioning of the Middle Jurassic Hugin Formation, Southern Viking Graben, North Sea," *Sedimentary Geology*, vol. 207, no. 1–4, pp. 1–21, 2008.
- [42] K. A. Eriksson and E. Simpson, "Precambrian tidal facies," in *Principles of Tidal Sedimentology*, R. A. Davis and R. W. Dalrymple, Eds., pp. 397–420, Springer, Heidelberg, Germany, 2012.
- [43] E. P. Kvale, A. W. Archer, and H. R. Johnson, "Daily, monthly, and yearly tidal cycles within laminated siltstones of the Mansfield Formation (Pennsylvanian) of Indiana," *Geology*, vol. 17, no. 4, pp. 365–368, 1989.
- [44] A. W. Archer and S. F. Greb, "Hypertidal facies from the pennsylvanian period: eastern and western interior Coal Basins, USA," in *Principles of Tidal Sedimentology*, R. A. Davis and R. W. Dalrymple, Eds., pp. 421–436, Springer, Heidelberg, Germany, 2012.
- [45] M. E. Tucker, *Sedimentary Petrology*, Blackwell, Oxford, UK, 3rd edition, 2001.
- [46] T. Chakraborty and S. Sensarma, "Shallow marine and coastal eolian quartz arenites in the Neoproterozoic-Palaeoproterozoic Karutola Formation, Dongargarh Volcano-sedimentary succession, central India," *Precambrian Research*, vol. 162, no. 1-2, pp. 284–301, 2008.
- [47] J. K. Warren, *Evaporites: Sediments, Resources and Hydrocarbons*, Springer, Berlin, Germany, 2006.
- [48] C. G. S. C. Kendall and J. Warren, "A review of the origin and setting of tepees and their associated fabrics," *Sedimentology*, vol. 34, no. 6, pp. 1007–1027, 1987.
- [49] H. Sano, T. Onoue, M. J. Orchard, and R. Martini, "Early Triassic peritidal carbonate sedimentation on a Panthalassan seamount: the Jesmond succession, Cache Creek Terrane, British Columbia, Canada," *Facies*, vol. 58, no. 1, pp. 113–130, 2012.
- [50] A. Aghaei, A. Mahboubi, R. Moussavi-Harami, C. Heubeck, and M. Nadjafi, "Facies analysis and sequence stratigraphy of an Upper Jurassic carbonate ramp in the Eastern Alborz range and Binalud Mountains, NE Iran," *Facies*, 2012.
- [51] Q. Ye and S. J. Mazzullo, "Dolomitization of lower Permian platform facies, Wichita Formation, north platform, Midland basin, Texas," *Carbonates and Evaporites*, vol. 8, no. 1, pp. 55–70, 1993.

- [52] E. C. Rankey and A. Berkeley, "Holocene carbonate tidal flats," in *Principles of Tidal Sedimentology*, R. A. Davis and R. W. Dalrymple, Eds., pp. 507–566, Springer, Heidelberg, Germany, 2012.
- [53] Z. J. Hughes, "Tidal channels on tidal flats and marshes," in *Principles of Tidal Sedimentology*, R. A. Davis and R. W. Dalrymple, Eds., pp. 269–300, Springer, Heidelberg, Germany, 2012.
- [54] S. Fagherazzi, L. Carniello, L. D'Alpaos, and A. Defina, "Critical bifurcation of shallow microtidal landforms in tidal flats and salt marshes," *Proceedings of the National Academy of Sciences of the United States of America*, vol. 103, no. 22, pp. 8337–8341, 2006.
- [55] G. M. Friedman, "Upper Cambrian-Lower Ordovician (Sauk) platform carbonates of the northern Appalachian (Gondwana) passive margin," *Carbonates and Evaporites*, vol. 9, no. 2, pp. 143–150, 1994.
- [56] P. B. Wignall and R. J. Twitchett, "Unusual intraclastic limestones in Lower Triassic carbonates and their bearing on the aftermath of the end-Permian mass extinction," *Sedimentology*, vol. 46, no. 2, pp. 303–316, 1999.
- [57] H. G. Reading and J. D. Collinson, "Clastic coastal," in *Sedimentary Environment and Facies*, H. G. Reading, Ed., pp. 154–231, Blackwell Scientific, Oxford, UK, 1996.
- [58] A. C. Kendall, "Evaporites," in *Facies Models: Responses to Sea Level Change*, R. G. Walker and N. P. James, Eds., pp. 374–409, Geological Association of Canada, Newfoundland, Canada, 1992.
- [59] A. C. Kendall, "Evaporites," in *Facies Models*, R. G. Walker, Ed., Geoscience Reprint Series 1, pp. 259–296, Geological Association of Canada, Newfoundland, Canada, 1982.
- [60] B. C. Schreiber, M. S. Roth, and M. L. Helman, "Recognition of primary facies characteristics of evaporites and the differentiation of these forms from diagenetic overprints," in *Proceedings of the Depositional and Diagenetic Spectra of Evaporates—A Core Workshop*, C. R. Handford, R. G. Loucks, and G. R. Davies, Eds., SEPM Core Workshop no. 3 Calgary, pp. 1–32, Society of Economic Paleontologists and Mineralogists, 1982.
- [61] A. Saleh, F. Al-Ruwaih, A. Al-Reda, and A. Gunatilaka, "A reconnaissance study of a clastic coastal sabkha in Northern Kuwait, Arabian Gulf," *Journal of Arid Environments*, vol. 43, no. 1, pp. 1–19, 1999.



Hindawi

Submit your manuscripts at
<http://www.hindawi.com>

